

# Kriging: Beyond Matérn

Pulong Ma

Statistical and Applied Mathematical Sciences Institute and Duke University  
79 T.W. Alexander Drive, P.O. Box 110207, Durham, NC 27709, USA  
pulong.ma@duke.edu

and

Anindya Bhadra

Department of Statistics, Purdue University  
250 N. University St., West Lafayette, IN 47907, USA  
bhadra@purdue.edu

## Abstract

The Matérn covariance function is a popular choice for prediction in spatial statistics and uncertainty quantification literature. A key benefit of the Matérn class is that it is possible to get precise control over the degree of differentiability of the process realizations. However, the Matérn class possesses exponentially decaying tails, and thus may not be suitable for modeling long range dependence. This problem can be remedied using polynomial covariances; however one loses control over the degree of differentiability of the process realizations, in that the realizations using polynomial covariances are either infinitely differentiable or not differentiable at all. We construct a new family of covariance functions using a scale mixture representation of the Matérn class where one obtains the benefits of both Matérn and polynomial covariances. The resultant covariance contains two parameters: one controls the degree of differentiability near the origin and the other controls the tail heaviness, independently of each other. Using a spectral representation, we derive theoretical properties of this new covariance including equivalence measures and asymptotic behavior of the maximum likelihood estimators under infill asymptotics. The improved theoretical properties in predictive performance of this new covariance class are verified via extensive simulations. Application using NASA's Orbiting Carbon Observatory-2 satellite data confirms the advantage of this new covariance class over the Matérn class, especially in extrapolative settings.

**Keywords:** Equivalence measures; Gaussian scale mixture; Long-range dependence; Prediction; Spectral density; XCO2 data.

## 1 Introduction

Kriging, a method for deriving the best spatial linear unbiased predictor in Gaussian process regression, is a term coined by Matheron (1963) in honor of the South African mining engineer D. G. Krige (Cressie, 1990). With origins in geostatistics, applications of kriging has permeated fields as diverse as spatial statistics (e.g., Banerjee et al., 2014; Cressie, 1993; Journel and Huijbregts, 1978; Matérn, 1960; Ripley, 1981; Stein, 1999), uncertainty quantification or UQ (e.g., Berger and Smith, 2019; Gu et al., 2018; Sacks et al., 1989; Santner et al., 2018) and machine learning (Williams and Rasmussen, 2006). Suppose  $\{Z(\mathbf{s}) \in \mathbb{R} : \mathbf{s} \in \mathcal{D} \subset \mathbb{R}^d\}$  is a stochastic process with a covariance function  $\text{cov}(Z(\mathbf{s}), Z(\mathbf{s} + \mathbf{h})) = C(\mathbf{h})$  that is solely a function of the increment  $\mathbf{h}$ . Then  $C(\cdot)$  is said to be second-order stationary (or weakly stationary). Further, if  $C(\cdot)$  is a function of  $\|\mathbf{h}\|$  with

$\|\cdot\|$  denoting the Euclidean norm, then  $C(\cdot)$  is called isotropic. If the process  $Z(\cdot)$  possesses a constant mean function and a weakly stationary (resp. isotropic) covariance function, the process  $Z(\cdot)$  is called weakly stationary (resp. isotropic). Further,  $Z(\cdot)$  is a Gaussian process (GP) if every finite-dimensional realization  $Z(\mathbf{s}_1), \dots, Z(\mathbf{s}_n)$  jointly follows a multivariate normal distribution for  $\mathbf{s}_i \in \mathcal{D}$  and every  $n$ .

The Matérn covariance function (Matérn, 1960) has been widely used in spatial statistics due to its flexible local behavior and nice theoretical properties (see, e.g., Stein, 1999) with increasing popularity in the UQ and machine learning literature (Guttorp and Gneiting, 2006). The Matérn covariance function is of the form:

$$\mathcal{M}(h) = \sigma^2 \frac{2^{1-\nu}}{\Gamma(\nu)} \left( \frac{\sqrt{2\nu}}{\phi} h \right)^\nu \mathcal{K}_\nu \left( \frac{\sqrt{2\nu}}{\phi} h \right), \quad (1)$$

where  $\sigma^2 > 0$  is the variance parameter,  $\phi > 0$  is the range parameter, and  $\nu > 0$  is the smoothness parameter that controls the differentiability of the associated random process. Here  $\mathcal{K}_\nu(\cdot)$  is the modified Bessel function of the second kind that satisfies  $\mathcal{K}_\nu(h) \asymp (\pi/(2h))^{1/2} \exp(-h)$  as  $h \rightarrow \infty$ , where  $f(x) \asymp g(x)$  denotes  $\lim_{x \rightarrow \infty} f(x)/g(x) = c \in (0, \infty)$ . Further, we use the notation  $f(x) \sim g(x)$  if  $c = 1$ . Thus, using this asymptotic expression of  $\mathcal{K}_\nu(h)$  for large  $h$  from Section 6 of Barndorff-Nielsen et al. (1982), the behavior of the Matérn covariance function is given by:

$$\mathcal{M}(h) \asymp h^{\nu-1/2} \exp \left\{ -\frac{\sqrt{2\nu}}{\phi} h \right\}, \quad h \rightarrow \infty.$$

Eventually, the  $\exp(-\sqrt{2\nu}h/\phi)$  term dominates, and the covariance decays exponentially for large  $h$ . This exponential decay may make it unsuitable for modeling some very long-range dependence. This problem with the Matérn covariance can be remedied by using covariance functions that decay polynomially, such as the generalized Wendland (Gneiting, 2002) and generalized Cauchy covariance functions (Gneiting, 2000; Gneiting and Schlather, 2004), but in using these polynomial covariance functions one loses a key benefit of the Matérn family: that of the degree of differentiability of the process realizations. Process realizations with a Matérn covariance function are exactly  $\lfloor \nu \rfloor$  times differentiable, whereas the realizations with a generalized Cauchy covariance function are either non-differentiable (very rough) or infinitely differentiable (very smooth), without any middle ground (Stein, 2005). The generalized Wendland covariance family also has limited flexibility near the origin compared to the Matérn class and has compact support (Gneiting, 2002).

Stochastic processes with power-law covariance for long-range dependence are ubiquitous in many scientific disciplines including geophysics, meteorology, hydrology, astronomy, agriculture and engineering; see Beran (1992) for a survey. In UQ studies, certain inputs may have little impact on output from a computer model, and these inputs are called *inert inputs*; see Chapter 7 of Santner et al. (2018) for detailed discussions. Long-range covariance functions can allow for large correlations among distant observations and hence are more suitable for modeling these inert inputs. Most often, computer model outputs can have different smoothness properties due to the behavior of the physical process to be modeled. Thus, long-range covariances with the possibility of controlling the differentiability of stochastic process realizations are very desirable

for modeling such output. In spatial statistics, long-range dependence has been studied in many works (e.g., Gay and Heyde, 1990; Gneiting, 2000; Haslett and Raftery, 1989). In the rest of the paper, we focus on modeling long-range dependence in spatial settings. As a motivating example, Figure 1 shows a 16-day repeat cycle of NASA’s Level 3 data product of the column-averaged carbon dioxide dry air mole fraction (XCO<sub>2</sub>) at 0.25° and 0.25° collected from the Orbiting Carbon Observatory-2 (OCO-2) satellite. The XCO<sub>2</sub> data are collected over long latitude bands and have large missing gaps between these latitude bands. Predicting the true process over these large missing gaps based on a spatial process model is challenging. If the covariance function only allows short-range dependence, the predicted true process will be predominated by the mean function in the spatial process model with the covariance function having negligible impact over these large missing gaps. However, if the covariance function can model long-range dependence, the predicted true process over these missing gaps will carry more information from distant locations where observations are available, presumably resulting in better prediction. Thus, it is of fundamental and practical interest to develop a covariance function to have long-range dependence without sacrificing the control over the smoothness behavior of the process realizations.

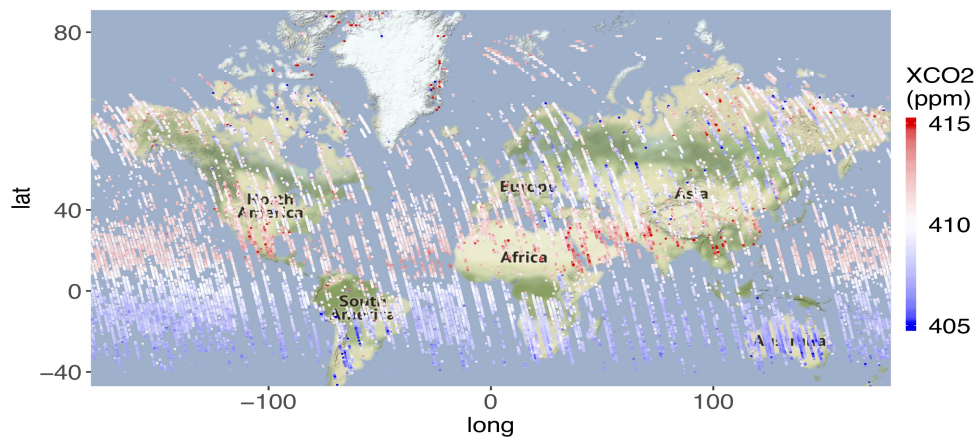


**Fig. 1.** XCO<sub>2</sub> data from June 1 to June 16, 2019. The units are parts per millions (ppm).

In this paper we propose a new family of covariance functions that bridges this gap between the Matérn covariance and polynomial covariances. The proposed covariance class is obtained by mixing the Matérn covariance over its range parameter  $\phi$ . This is done by recognizing the Bessel function in the Matérn covariance function as proportional to the normalizing constant of the generalized inverse Gaussian distribution (Barndorff-Nielsen, 1977, 1978), which then allows analytically tractable calculations with respect to a range of choices for mixing densities, resulting in valid covariance functions with varied features. Apart from this technical innovation, the key benefit is that this mixing does not affect the origin behavior and thus allows one to retain the precise control over the smoothness of process realizations as in Matérn. However, the tail is inflated due to mixing, and, in fact, the mixing distribution can be chosen in a way so that the tail of the resultant covariance function displays regular variation, with precise control over the tail decay parameter  $\alpha$ . A function  $f(\cdot)$  is said to have a regularly decaying right tail with index  $\alpha$  if it satisfies  $f(x) \asymp x^{-\alpha}L(x)$  as  $x \rightarrow \infty$  for some  $\alpha > 0$  where  $L(\cdot)$  is a slowly varying function at infinity with the property  $\lim_{x \rightarrow \infty} L(tx)/L(x) = 1$  for all  $t \in (0, \infty)$  (Bingham et al., 1989). Unlike a generalized Cauchy covariance function, this new covariance class is obtained without

sacrificing the control over the degree of differentiability of the process, which is still controlled solely by  $\nu$ , and the resulting process is still exactly  $\lfloor \nu \rfloor$  times differentiable, independent of  $\alpha$ . Moreover, regular variation is preserved under several commonly used transformations, such as sums or products. Thus, it is possible to exploit these properties of regular variation to derive new covariance functions with similar features from the original covariance function that is obtained via a mixture of the Matérn class.

The rest of the paper is organized as follows. Section 2 begins with the construction of the proposed covariance function as a mixture of the Matérn covariance function over its range parameter. We verify that such construction indeed results in a valid covariance function. The behaviors of this covariance function near the origin and in the tails are characterized by two distinct parameters, which in turn control over the smoothness and the degree of long-range dependence, respectively. Section 3 presents the main theoretical results for the new covariance function. We first derive the spectral representation of this new covariance and characterize its high-frequency behavior, and then show theoretical properties concerning equivalence classes under Gaussian measures and asymptotic normality of the maximum likelihood estimators. The resultant theory is extensively verified via simulations in Section 4. In Section 5, we use this new covariance function to analyze NASA's OCO-2 data, and demonstrate better prediction results over the Matérn covariance function. Section 6 concludes with some discussions for future investigations.

## 2 A New Covariance Class as a Mixture of the Matérn Class

Our starting point in mixing over the range parameter  $\phi$  in the Matérn covariance function is the correspondence between form of the Matérn covariance function and the normalizing constant of the generalized inverse Gaussian distribution of Barndorff-Nielsen (1977). The generalized inverse Gaussian distribution has density on  $(0, \infty)$  given by:

$$\pi_{GIG}(x) = \frac{(a/b)^{p/2}}{2\mathcal{K}_p(\sqrt{ab})} x^{(p-1)} \exp\{-(ax + b/x)/2\}; \quad a, b > 0, p \in \mathbb{R}.$$

Thus,

$$\mathcal{K}_p(\sqrt{ab}) = \frac{1}{2}(a/b)^{p/2} \int_0^\infty x^{(p-1)} \exp\{-(ax + b/x)/2\} dx.$$

Take  $a = \phi^{-2}, b = 2\nu h^2$  and  $p = \nu$ . Then we have the following representation of the Matérn covariance function with range parameter  $\phi$  and smoothness parameter  $\nu$ :

$$\begin{aligned} \mathcal{M}(h) &= \sigma^2 \frac{2^{1-\nu}}{\Gamma(\nu)} \left( \frac{\sqrt{2\nu}}{\phi} h \right)^\nu \mathcal{K}_\nu \left( \frac{\sqrt{2\nu}}{\phi} h \right) \\ &= \sigma^2 \frac{2^{1-\nu}}{\Gamma(\nu)} \left( \frac{\sqrt{2\nu}h}{\phi} \right)^\nu \frac{1}{2} \left( \frac{1}{\sqrt{2\nu}h\phi} \right)^\nu \int_0^\infty x^{(\nu-1)} \exp\{-(x/\phi^2 + 2\nu h^2/x)/2\} dx \\ &= \frac{\sigma^2}{2^\nu \phi^{2\nu} \Gamma(\nu)} \int_0^\infty x^{(\nu-1)} \exp\{-(x/\phi^2 + 2\nu h^2/x)/2\} dx. \end{aligned}$$

Thus, the mixture over  $\phi^2$  with respect to a mixing density  $\pi(\phi^2)$  can be written as

$$\begin{aligned} C(h) &:= \int_0^\infty \mathcal{M}(h) \pi(\phi^2) d\phi^2 = \int_0^\infty \left[ \frac{\sigma^2}{2^v \phi^{2v} \Gamma(v)} \int_0^\infty x^{(v-1)} \exp\{-(x/\phi^2 + 2vh^2/x)/2\} dx \right] \pi(\phi^2) d\phi^2 \\ &= \frac{\sigma^2}{2^v \Gamma(v)} \int_0^\infty x^{(v-1)} \left[ \int_0^\infty \phi^{-2v} \exp\{-x/(2\phi^2)\} \pi(\phi^2) d\phi^2 \right] \exp(-vh^2/x) dx. \end{aligned} \quad (2)$$

The inner integral may be recognized as a mixture of gamma integrals (by change of variable  $u = \phi^{-2}$ ), which is analytically tractable for many choices of  $\pi(\phi^2)$ ; see for example the chapter on gamma integrals in Abramowitz and Stegun (1965). More importantly, as we show below, the parameters of the mixing density  $\pi(\phi^2)$  can be chosen to achieve precise control over certain features of the resulting covariance function. Our first result is as follows, with proof given in Section S.1 of the Supplementary Material.

**THEOREM 1.** *Let  $X \sim \mathcal{IG}(a, b)$  denote an inverse gamma random variable using the shape–scale parameterization with density  $\pi_{\mathcal{IG}}(x) = \{b^a / \Gamma(a)\} x^{-a-1} \exp(-b/x)$ ;  $a, b > 0$ . Assume that  $(\phi^2) \sim \mathcal{IG}(\alpha, \beta/2)$  and that  $\mathcal{M}(h)$  is the Matérn covariance function in Equation (1). Then  $C(h) = \int_0^\infty \mathcal{M}(h) \pi(\phi^2) d\phi^2$  is a valid covariance function on  $\mathbb{R}^d$  with the following form:*

$$C(h) = \frac{\sigma^2 \beta^\alpha \Gamma(v + \alpha)}{\Gamma(v) \Gamma(\alpha)} \int_0^\infty x^{(v-1)} (x + \beta)^{-(v+\alpha)} \exp(-vh^2/x) dx, \quad (3)$$

where  $\sigma^2 > 0$  is the variance parameter,  $\alpha > 0$  is called the tail decay parameter,  $\beta > 0$  is called the scale parameter, and  $v > 0$  is called the smoothness parameter.

Having established the resultant mixture as a valid covariance function, one may take a closer look at its properties. To begin, although the final form of  $C(h)$  involves an integral, and thus may not appear to be in closed form at a first glance, the situation is indeed not too different from that of Matérn, where the associated Bessel function is available in an algebraically closed form only for certain special cases; otherwise it is available as an integral. In addition, this representation of  $C(h)$  is sufficient for numerically evaluating the covariance function as a function of  $h$  via either quadrature or Monte Carlo methods. Additionally, with a certain change of variable, the above integral can be identified as belonging to a certain class of special functions that can be computed efficiently. More precisely, we have the following elegant representation for the new covariance function.

**COROLLARY 1.** *The proposed covariance function in Equation (3) can also be represented in terms of the confluent hypergeometric function of the second kind:*

$$C(h) = \frac{\sigma^2 \Gamma(v + \alpha)}{\Gamma(v)} \mathcal{U}(\alpha, 1 - v, vh^2/\beta), \quad (4)$$

where  $\alpha > 0, \beta > 0$  and  $v > 0$ .

*Proof.* By making the change of variable  $x = \beta/t$ , standard calculation yields that

$$C(h) = \frac{\sigma^2 \Gamma(v + \alpha)}{\Gamma(v) \Gamma(\alpha)} \int_0^\infty t^{\alpha-1} (t + 1)^{-(v+\alpha)} \exp\{-vh^2 t/\beta\} dt.$$

Thus, the conclusion follows by recognizing the form of the confluent hypergeometric function of the second kind  $\mathcal{U}(a, b, c)$  from Chapter 13.2 of Abramowitz and Stegun (1965).  $\square$

Equation (4) provides a convenient way to evaluate the new covariance function, since efficient numerical calculation of the confluent hypergeometric function is implemented in various libraries such as the GNU scientific library (Galassi et al., 2002) and softwares including R and MATLAB, facilitating its practical deployment. The Matérn covariance function is sometimes parameterized differently. The mixing density can be chosen accordingly to arrive at results identical to ours. For instance, with parameterization of the Matérn class given in Stein (1999), a gamma mixing density with shape parameter  $\alpha$  and rate parameter  $\beta/2$  would lead to an alternative route to the same representation of the new covariance class. The limiting case of the Matérn class is the squared exponential (or Gaussian) covariance function when the smoothness parameter in Equation (1) goes to  $\infty$ . Mixing over the inverse gamma distribution in Theorem 1 yields a special case of the generalized Cauchy covariance function.

Besides the computational convenience, the new covariance function in Equation (3) also allows us to make precise statements concerning the origin and tail behaviors of the resultant mixture. This is clearly more important, since for stationary random fields, the short-range (local) behavior is determined by the differentiability of the covariance function near origin, while the long-range behavior is determined by the tail behavior of the covariance function. The next theorem makes the origin and tail behaviors explicit with proof given in Section S.2 of the Supplementary Material.

**THEOREM 2.** *The covariance function  $C(h)$  has the following two properties:*

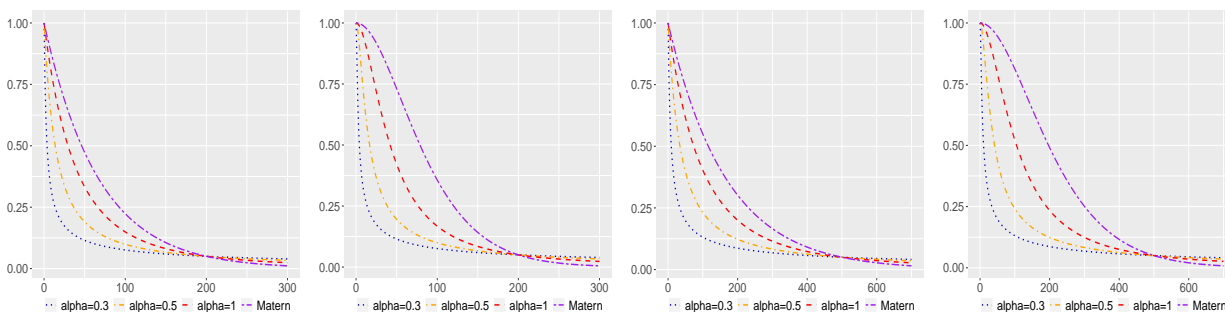
- (a) **Origin behavior:**  $C(h)$  has the same origin behavior as the Matérn covariance function given in Equation (1).
- (b) **Tail behavior:**  $C(h) \sim \frac{\sigma^2 2^{\alpha-1} \Gamma(\nu+\alpha)}{(\nu/\beta)^\alpha \Gamma(\nu)} |h|^{-2\alpha} L(h^2)$  as  $h \rightarrow \infty$ , where  $L(x)$  is a slowly varying function at  $\infty$  of the form  $L(x) = \left(\frac{x}{x+\beta/(2\nu)}\right)^{\nu+\alpha}$ .

A weakly stationary process on  $\mathbb{R}^d$  is  $k$ -times differentiable if its covariance function has  $2k$  derivatives at the origin (Stein, 1999, Section 2.4). A random process generated by the new covariance function with smoothness parameter  $\nu$  is  $\lfloor \nu \rfloor$  times differentiable in the mean-square sense. The local behavior of this new covariance function is very flexible in the sense that the parameter  $\nu$  can allow for any degree of differentiability of a weakly stationary random process in the same way as the Matérn class. However, its tail behavior is quite different from that of the Matérn class, since the new covariance function  $C(h)$  has a polynomial tail that decays slower than the exponential tail in the Matérn covariance function. This is natural since mixture inflates the tails in general, and in our particular case, changes the exponential decay to a polynomial one. The rate of tail decay is controlled by the parameter  $\alpha$ . Thus, this new covariance class may be more suitable for very long range dependence which an exponentially decaying covariance function may fail to capture. Moreover, the control over the degree of smoothness of the process realization is not lost. Theorem 2 also establishes a very desirable property that the degrees of differentiability near origin and the rate of decay of the tail for the new covariance function  $C(h)$  are controlled

by two different parameters,  $\nu$  and  $\alpha$ , independently of each other. Each of these parameters can allow any degrees of flexibility.

To get a clear picture of the difference between the new covariance class and the Matérn class, we fix the *effective range* (ER) at 200 and 500, where ER is defined as the distance at which a correlation function has value approximately 0.05. Then we find the corresponding scale parameter  $\beta$  such that the new covariance function has ER at 200 and 500 under different smoothness parameters  $\nu \in \{0.5, 2.5\}$  and different tail decay parameters  $\alpha \in \{0.3, 0.5, 1\}$ . For the Matérn class, we find the corresponding range parameter  $\phi$  such that the Matérn correlation function has ER at 200 and 500 under smoothness parameters 0.5 and 2.5. These correlation functions are visualized in Figure 2. Clearly we can see different smoothness behaviors near the origin. As the new covariance class has a polynomial tail, its correlation drops much faster than the Matérn class in order to reach the same correlation 0.05 at the same effective range. If  $\alpha$  is smaller, the new correlation function has a heavier tail, and hence it drops more quickly to reach the correlation 0.05 at the same effective range. After the effective range, the new covariance function with a smaller  $\alpha$  decays slower than those with larger  $\alpha$ . As the Matérn class has an exponentially decaying tail, it decays much faster than the new covariance class. This is indicated by the behavior of the Matérn covariance function after the ER compared to the new covariance class.

In Figure 3, we show the realizations from zero mean Gaussian processes with the new covariance class and the Matérn class under different parameter settings. When the distance is within the effective range, the Matérn covariance function results in more large correlations than the new covariance function. This makes the process realizations from the Matérn class smoother even though both the Matérn class and the new covariance class are fixed at the same value for the smoothness parameter. For the new covariance class, if  $\alpha$  has a smaller value, the corresponding correlation function has more small values within the effective range. This makes the process realizations under the new covariance class look rougher. As we expect, when the effective range and the tail decay parameter are fixed, the process realizations under the new covariance class look smoother for a larger value of the smoothness parameter.



(a)  $\nu = 0.5, ER = 200$       (b)  $\nu = 2.5, ER = 200$       (c)  $\nu = 0.5, ER = 500$       (d)  $\nu = 2.5, ER = 500$

**Fig. 2.** Correlation functions for the new covariance class and the Matérn class. The panels (a) and (b) show the correlation functions with the effective range (ER) at 200. The panels (c) and (d) show the correlation functions with the effective range (ER) at 500. ER is defined as the distance at which correlation is approximately 0.05.

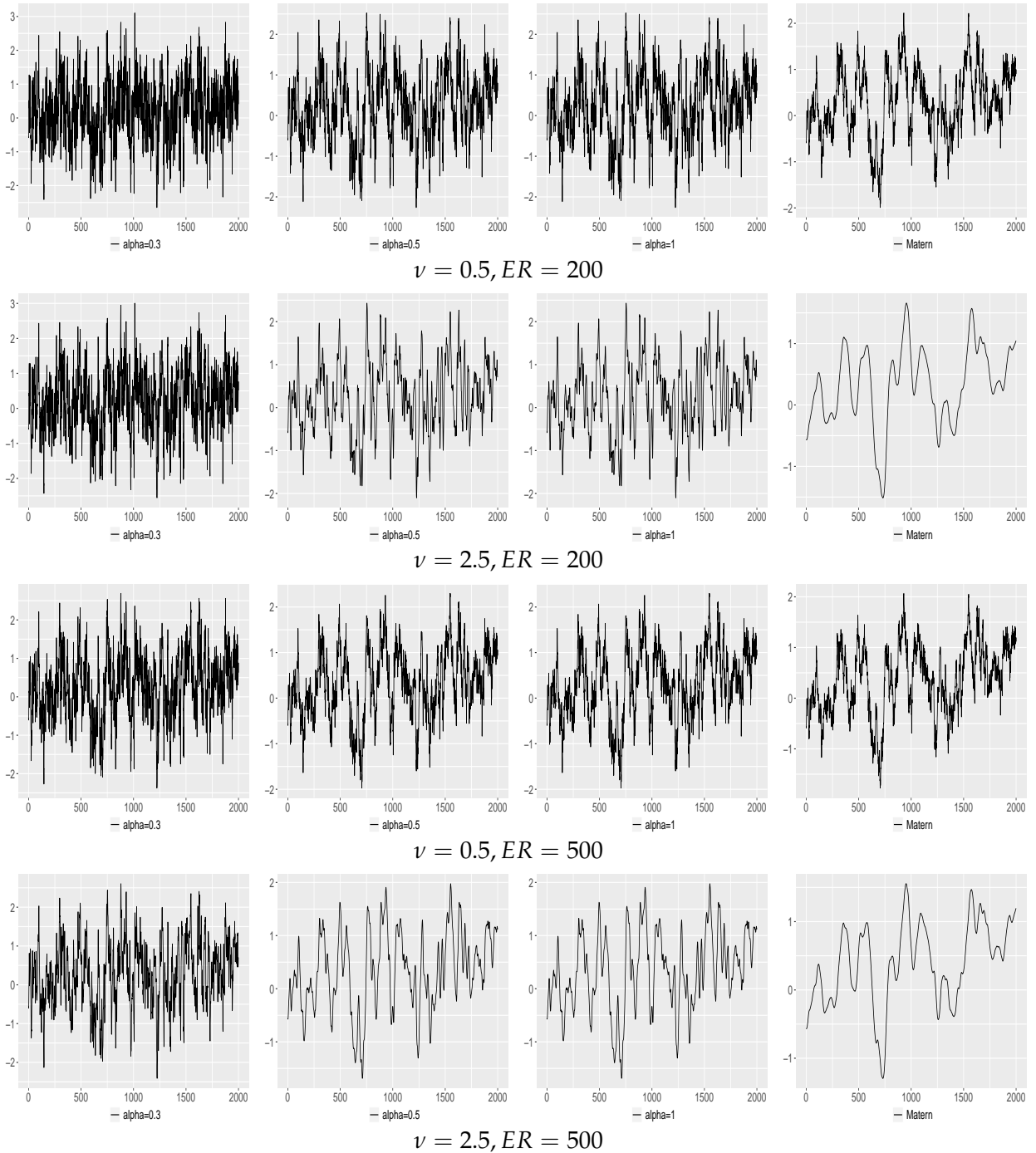


**Fig. 3.** Realizations over 2000 regular grid points in the domain  $[0, 2000]$  from zero mean Gaussian processes with the new covariance function model and the Matérn covariance function model under different parameter settings. The realizations from the new covariance are shown in the first three columns and those from the Matérn covariance are shown in the last column. For the first two rows, the effective range (ER) is fixed at 200. For the last two rows, the effective range is fixed at 500. ER is defined as the distance at which correlation is approximately 0.05.

### 3 Theoretical Properties of the Proposed Covariance Class

For an isotropic random field, the property of a covariance function can be characterized by its spectral density. By Bochner's Theorem (Bochner, 1933), there is a dual form between an isotropic covariance function and its spectral density in  $\mathbb{R}^d$  if  $\int_0^\infty h^{d-1}|C(h)|dh < \infty$ , see also Section 2.10 of Stein (1999). Given the existence of the corresponding spectral density, the origin behavior (low frequency) of the spectral density of a covariance characterizes the large-scale variation of the random process, while its tail behavior (high frequency) characterizes the small-scale variation.

The spectral density of the new covariance function is finite for  $\alpha > d/2$  and infinite for  $\alpha \in (0, d/2]$ . The following theorem gives the spectral density of the new covariance function in Equation (3) and characterizes the tail behavior of the spectral density, with its proof given in Section S.3 of the Supplementary Material.

**THEOREM 3 (Spectral density).** *If  $\alpha > d/2$ , the new covariance function in Equation (3) admits the following spectral density:*

$$f(\omega) = \frac{\sigma^2 2^{v-\alpha} \nu^\nu \beta^\alpha}{\pi^{d/2} \Gamma(\alpha)} \int_0^\infty (2\nu\phi^{-2} + \omega^2)^{-\nu-d/2} \phi^{-2(\nu+\alpha+1)} \exp\{-\beta/(2\phi^2)\} d\phi^2, \quad (5)$$

with the tail behavior

$$f(\omega) \sim \frac{\sigma^2 2^{2\nu} \nu^\nu \Gamma(\nu + \alpha)}{\pi^{d/2} \beta^\nu \Gamma(\alpha)} \omega^{-(2\nu+d)} L(\omega^2), \quad \omega \rightarrow \infty,$$

where  $L(x) = \left\{ \frac{x}{x + \beta/(2\nu)} \right\}^{\nu+d/2}$  is a slowly varying function at  $\infty$ .

The spectral density of the Matérn class is proportional to  $\omega^{-(2\nu+d)}$  for large  $\omega$ . By mixing over the range parameter with an inverse gamma mixing density, the high-frequency behavior of the resultant covariance class is proportional to the product of the high-frequency term of the Matérn class and a slowly varying function  $L(\omega^2)$ . This slowly varying function does not change the high-frequency behavior. When the spectral density is finite at any frequency, i.e.,  $\alpha > d/2$ , this is another an argument on why the origin behavior of the new covariance class is controlled in the same way as the that of the Matérn class. In what follows, the theoretical results are established based on the condition that  $\alpha > d/2$ .

It is well understood that the spectral density of the Matérn class is well-behaved at high frequencies, equipped with the phenomenon in geostatistics known as ‘‘screening effect’’ (Journel and Huijbregts, 1978), which means that nearby observations yield a good approximation to the optimal linear predictor of a spatial process based on a large set of observations. The screening effect has been studied extensively by Stein (2002, 2011, 2015) who gives conditions on when it holds and does not hold for isotropic random fields. The spectral density of the new covariance class is well-behaved at high frequencies in a way similar to the Matérn class. Notice that for the Matérn class, the following condition holds for any finite  $R > 0$ ,

$$\lim_{|\omega| \rightarrow \infty} \sup_{|u| < R} \left| \frac{f(\omega + u)}{f(\omega)} - 1 \right| = 0.$$

This condition effectively implies that the spectral density of the Matérn class at high frequencies changes by a negligible amount with a modest change in frequency (Stein, 2011, 2015). The spectral density of the new covariance at high frequencies differs from that of the Matérn class by a slowly varying multiplicative function and a multiplicative constant that does not depend on frequency. Thus, the spectral density of the new covariance class also displays the screening effect.

### 3.1 Equivalence Results

As discussed by Zhang (2004), the equivalence of probability measures has important applications to statistical inferences on parameter estimation and prediction. Let  $\mathcal{P}_i, i = 1, 2$ ; be two probability measures corresponding to the spectral density  $f_i$  for stationary Gaussian process with mean zero in  $\mathbb{R}^d$ . If  $\mathcal{P}_1$  is equivalent to  $\mathcal{P}_2$ , then  $\mathcal{P}_1$  cannot be correctly distinguished from  $\mathcal{P}_2$  with  $\mathcal{P}_1$  with probability 1 regardless of what is observed. Let  $\{\mathcal{P}_\theta : \theta \in \Theta\}$  be a sequence of distributions on the parameter space  $\Theta$  and  $\hat{\theta}_n$  be a sequence of estimators. Then  $\hat{\theta}_n$  cannot be consistent estimators of  $\theta$  for all  $\theta \in \Theta$  under the infill asymptotics (or fixed domain asymptotics), where the domain is fixed (bounded) and the locations of observations get denser as the number of observations increases. The second application of equivalence measures concerns the asymptotic efficiency of predictors that is discussed in Section 3.3.

The tail behavior of the spectral densities can be used to check the equivalence of probability measures generated by stationary Gaussian random fields. If for some  $\lambda > 0$  and for some finite  $c \in \mathbb{R}$ , one has

$$0 < f_1(\boldsymbol{\omega})|\boldsymbol{\omega}|^\lambda < \infty \quad \text{as } |\boldsymbol{\omega}| \rightarrow \infty, \quad \text{and} \quad (6)$$

$$\int_{|\boldsymbol{\omega}|>c} \left\{ \frac{f_1(\boldsymbol{\omega}) - f_2(\boldsymbol{\omega})}{f_1(\boldsymbol{\omega})} \right\}^2 d\boldsymbol{\omega} < \infty, \quad (7)$$

then the two Gaussian measures  $\mathcal{P}_1$  and  $\mathcal{P}_2$  are equivalent. For isotropic Gaussian random fields, the condition in Equation (7) can be expressed as

$$\int_c^\infty \omega^{d-1} \left\{ \frac{f_1(\omega) - f_2(\omega)}{f_1(\omega)} \right\}^2 d\omega < \infty. \quad (8)$$

The details of equivalence of Gaussian measures and the condition for equivalence can be found in a series of works (Stein, 1988, 1993, 1999; Stein and Handcock, 1989). Our first result on equivalence of two Gaussian measures under the new covariance class is given in Theorem 4 with its proof given in Section S.4 of the Supplementary Material.

**THEOREM 4 (Equivalence measures).** *Assume that  $\alpha > d/2$ . Let  $f_i$  be the spectral density of the covariance  $C(h; \nu, \alpha_i, \beta_i, \sigma_i^2)$  for  $i = 1, 2$ . Then  $\mathcal{P}_1$  and  $\mathcal{P}_2$  are equivalent on the paths of  $\{Z(\mathbf{s}) : \mathbf{s} \in \mathcal{D}\}$  for any bounded infinite set  $\mathcal{D} \subset \mathbb{R}^d$  with  $d = 1, 2, 3$  if and only if*

$$\frac{\sigma_1^2 \Gamma(\nu + \alpha_1)}{\beta_1^\nu \Gamma(\alpha_1)} = \frac{\sigma_2^2 \Gamma(\nu + \alpha_2)}{\beta_2^\nu \Gamma(\alpha_2)}. \quad (9)$$

*Notice that if these two covariances are further assumed to have the same tail decay parameter  $\alpha := \alpha_1 = \alpha_2$ ,*

the above condition becomes  $\sigma_1^2 \beta_1^{-\nu} = \sigma_2^2 \beta_2^{-\nu}$ .

An immediate consequence of Theorem 4 is that for fixed  $\nu$ ; the tail decay parameter  $\alpha$ , the scale parameter  $\beta$  and the variance parameter  $\sigma^2$  cannot be estimated consistently under the infill asymptotics. Instead, the quantity  $\sigma^2 \beta^{-\nu} \Gamma(\nu + \alpha) / \Gamma(\alpha)$  is consistently estimable and has been referred to as the *microergodic parameter*. We refer the readers to page 163 of Stein (1999) for the definition of microergodicity. Similarly, for fixed  $\nu$  and  $\alpha$ , the scale parameter  $\beta$  and the variance parameter  $\sigma^2$  cannot be estimated consistently. Instead, the microergodic parameter  $\sigma^2 \beta^{-\nu}$  can be estimated consistently. In the next section, we establish the asymptotic properties of maximum likelihood estimation associated with the microergodic parameter.

Theorem 4 gives the result on equivalence measures within the new covariance class. The new covariance can allow the same smoothness behavior as the Matérn class, but it has a polynomially decaying tail that is quite different from the Matérn class. One may ask whether there is an analogous result on the Gaussian measures under the new covariance class and the Matérn class. Theorem 5 provides an answer to this question, with its proof given in Section S.5 of the Supplementary Material.

**THEOREM 5 (Equivalence measures with Matérn).** *Assume that  $\alpha > d/2$ . Let  $f_1$  be the spectral density of the new covariance function  $C(h; \nu, \alpha, \beta, \sigma_1^2)$  and  $f_2$  be the spectral density of the Matérn covariance function  $\mathcal{M}(h; \nu, \phi, \sigma_2^2)$ . If*

$$\sigma_1^2 (\beta/2)^{-\nu} \Gamma(\nu + \alpha) / \Gamma(\alpha) = \sigma_2^2 \phi^{-2\nu}, \quad (10)$$

then  $\mathcal{P}_1$  and  $\mathcal{P}_2$  are equivalent on the paths of  $\{Z(\mathbf{s}) : \mathbf{s} \in \mathcal{D}\}$  for any bounded infinite set  $\mathcal{D} \subset \mathbb{R}^d$  with  $d = 1, 2, 3$

Theorem 5 gives the conditions under which the Gaussian measures under the new covariance class and the Matérn class are equivalent. If the condition in Equation (10) is satisfied, the Gaussian measure under the new covariance class cannot be distinguished from the Gaussian measure under the Matérn class, regardless of what is observed.

Based on Theorem 4, one can study the asymptotic properties of the microergodic parameter  $\sigma^2 \beta^{-\nu} \Gamma(\nu + \alpha) / \Gamma(\alpha)$ . In Section 3.2, the microergodic parameter  $\sigma^2 \beta^{-\nu} \Gamma(\nu + \alpha) / \Gamma(\alpha)$  can be shown to be consistently estimated under infill asymptotics for a Gaussian process under the new covariance model with known  $\nu$ . Moreover, one can show that this microergodic parameter converges to a normal distribution.

### 3.2 Asymptotic Normality

Let  $\{Z(\mathbf{s}) : \mathbf{s} \in \mathcal{D}\}$  be a zero mean Gaussian process with the covariance function  $C(h; \nu, \alpha, \beta, \sigma^2)$ , where  $\mathcal{D} \subset \mathbb{R}^d$  is a bounded subset of  $\mathbb{R}^d$  with  $d = 1, 2, 3$ . Let  $\mathbf{Z}_n := (Z(\mathbf{s}_1), \dots, Z(\mathbf{s}_n))^\top$  be a partially observed realization of the process  $Z(\cdot)$  at  $n$  distinct locations in  $\mathcal{D}$ , denoted by  $\mathcal{D}_n := \{\mathbf{s}_1, \dots, \mathbf{s}_n\}$ . Then the log-likelihood function is

$$\ell_n(\sigma^2, \boldsymbol{\theta}) = -\frac{1}{2} \left\{ n \log(2\pi\sigma^2) + \log |\mathbf{R}_n(\boldsymbol{\theta})| + \frac{1}{\sigma^2} \mathbf{Z}_n^\top \mathbf{R}_n^{-1}(\boldsymbol{\theta}) \mathbf{Z}_n \right\}, \quad (11)$$

where  $\boldsymbol{\theta} := \{\alpha, \beta\}$  and  $\mathbf{R}_n(\boldsymbol{\theta}) = [R(\|\mathbf{s}_i - \mathbf{s}_j\|; \boldsymbol{\theta})]_{i,j=1,\dots,n}$  is an  $n \times n$  correlation matrix with the correlation function  $R(h) := C(h)/\sigma^2$ .

In what follows,  $\nu$  is assumed to be known and fixed. Let  $\hat{\sigma}_n^2$  and  $\hat{\boldsymbol{\theta}}_n$  be the maximum likelihood estimators (MLE) for  $\sigma^2$  and  $\boldsymbol{\theta}$  by maximizing the log-likelihood function in Equation (11). To show the consistency and asymptotic results for the microergodic parameter, we first obtain an estimator for  $\sigma^2$  when  $\boldsymbol{\theta}$  is fixed:

$$\hat{\sigma}_n^2 := \operatorname{argmax}_{\sigma^2} \ell_n(\sigma^2, \boldsymbol{\theta}) = \mathbf{Z}_n^\top \mathbf{R}_n^{-1}(\boldsymbol{\theta}) \mathbf{Z}_n / n.$$

Then, let  $\hat{c}_n(\boldsymbol{\theta})$  be the maximum likelihood estimator of  $c(\boldsymbol{\theta}) := \sigma^2 \beta^{-\nu} \Gamma(\nu + \alpha) / \Gamma(\alpha)$ , as a function of  $\boldsymbol{\theta}$ , given by

$$\hat{c}_n(\boldsymbol{\theta}) = \frac{\hat{\sigma}_n^2 \Gamma(\nu + \alpha)}{\beta^\nu \Gamma(\alpha)} = \frac{\mathbf{Z}_n^\top \mathbf{R}_n^{-1}(\boldsymbol{\theta}) \mathbf{Z}_n \Gamma(\nu + \alpha)}{n \beta^\nu \Gamma(\alpha)}.$$

We have the following result on the asymptotic properties of  $\hat{c}_n(\boldsymbol{\theta})$  for arbitrarily fixed values  $\alpha > 0$  and  $\beta > 0$  under the infill asymptotics, with its proof given in Section S.6 of the Supplementary Material.

**THEOREM 6 (Asymptotics of the MLE).** *Let  $\mathcal{D}_n$  be an increasing sequence of subsets of a bounded domain  $\mathcal{D}$ . Assume that  $\nu$  is fixed. Then under  $C(h; \nu, \alpha_0, \beta_0, \sigma_0^2)$ , as  $n \rightarrow \infty$ , for any fixed  $\alpha > d/2$  and  $\beta > 0$ ,*

- (a)  $\hat{c}_n(\boldsymbol{\theta}) \xrightarrow{a.s.} c(\boldsymbol{\theta}_0)$ ,
- (b)  $\sqrt{n} \{\hat{c}_n(\boldsymbol{\theta}) - c(\boldsymbol{\theta}_0)\} \xrightarrow{\mathcal{L}} \mathcal{N}(0, 2[c(\boldsymbol{\theta}_0)]^2)$ ,

where  $c(\boldsymbol{\theta}_0) = \sigma_0^2 \beta_0^{-\nu} \Gamma(\nu + \alpha_0) / \Gamma(\alpha_0)$ .

Theorem 6 implies that the estimator  $\hat{c}_n(\boldsymbol{\theta})$  of the microergodic parameter converges to the true microergodic parameter, almost surely, when the number of observations tends to infinity in a fixed and bounded domain. This result holds true for any value of  $\boldsymbol{\theta}$ . As will be shown, if one replaces  $\boldsymbol{\theta}$  with its maximum likelihood estimator in  $\hat{c}_n(\boldsymbol{\theta})$ , this conclusion is true as well. The second statement of Theorem 6 indicates that  $\hat{c}_n(\boldsymbol{\theta})$  converges to a normal distribution.

A key fact is that the above theorem holds true for arbitrarily fixed  $\boldsymbol{\theta}$ . A more practical situation is to estimate  $\boldsymbol{\theta}$  and  $\sigma^2$  by maximizing the log-likelihood (11). For notational convenience, we use  $c(\alpha, \beta)$  instead of  $c(\boldsymbol{\theta})$  to denote the microergodic parameter when needed. We discuss three situations. In the first situation, we consider joint estimation of  $\beta$  and  $\sigma^2$  for fixed  $\alpha$ . The MLE of  $\beta$  will be denoted by  $\hat{\beta}_n$ , and the MLE of the microergodic parameter is  $\hat{c}_n(\alpha, \hat{\beta}_n)$ . In the second situation, we consider joint estimation of  $\alpha$  and  $\sigma^2$  for fixed  $\beta$ . The MLE of  $\alpha$  will be denoted by  $\hat{\alpha}_n$  and the MLE of the microergodic parameter is  $\hat{c}_n(\hat{\alpha}_n, \beta)$ . In the third situation, we consider joint estimation of all parameters  $\alpha, \beta, \sigma^2$ . Note that the MLEs of either  $\alpha$  or  $\beta$  (or both) are typically computed numerically, since there is no closed-form expression. Theorem 6 can be used to show that  $\hat{c}_n(\hat{\boldsymbol{\theta}}_n)$  has the same asymptotic properties as  $\hat{c}_n(\boldsymbol{\theta})$  for any fixed  $\boldsymbol{\theta}$ . The following lemma is needed to prove the asymptotic behavior of  $\hat{c}_n(\alpha, \hat{\beta}_n)$  and  $\hat{c}_n(\hat{\alpha}_n, \beta)$  under infill asymptotics, with its proof given in Section S.7 of the Supplementary Material.

**LEMMA 1.** Suppose that  $d$  is the dimension of the domain  $\mathcal{D}$  and  $\mathbf{Z}_n$  is a vector of  $n$  observations in  $\mathcal{D}$ . For any  $\alpha_1 < \alpha_2$  and  $\beta_1 < \beta_2$  with  $\alpha_i \in [\alpha_L, \alpha_U]$  and  $\beta_i \in [\beta_L, \beta_U]$ ,  $i = 1, 2$ , where  $\alpha_L > d/2$  and  $\beta_L > 0$ , we have the following results:

(a)  $\hat{c}_n(\alpha, \beta_1) \leq \hat{c}_n(\alpha, \beta_2)$  for any fixed  $\alpha > d/2$ .

(b)  $\hat{c}_n(\alpha_1, \beta) \geq \hat{c}_n(\alpha_2, \beta)$  for any fixed  $\beta > 0$ .

**THEOREM 7 (Asymptotics of the MLE: joint estimation).** Let  $\mathcal{D}_n$  be an increasing sequence of subsets of  $\mathcal{D}$ . Assume that  $d/2 < \alpha_L < \alpha_U$  and  $0 < \beta_L < \beta_U$ . Let  $\hat{c}_n(\alpha, \hat{\beta}_n)$  be the MLE of the microergodic parameter  $c(\alpha_0, \beta_0)$  over  $[\beta_L, \beta_U] \times (0, \infty)$  for any fixed  $\alpha > 0$ ,  $\hat{c}_n(\hat{\alpha}_n, \beta)$  be the MLE of the microergodic parameter  $c(\alpha_0, \beta_0)$  over  $[\alpha_L, \alpha_U] \times (0, \infty)$  for any fixed  $\beta > 0$ , and  $\hat{c}_n(\hat{\alpha}_n, \hat{\beta}_n)$  be the MLE of the microergodic parameter  $c(\alpha_0, \beta_0)$  over  $[\alpha_L, \alpha_U] \times [\beta_L, \beta_U] \times (0, \infty)$ . Then under  $C(h; \nu, \alpha_0, \beta_0, \sigma_0^2)$ , as  $n \rightarrow \infty$ , the following results can be established:

(a)  $\hat{c}_n(\alpha, \hat{\beta}_n) \xrightarrow{a.s.} c(\boldsymbol{\theta}_0)$  and  $\sqrt{n} \{ \hat{c}_n(\alpha, \hat{\beta}_n) - c(\boldsymbol{\theta}_0) \} \xrightarrow{\mathcal{L}} \mathcal{N}(0, 2[c(\boldsymbol{\theta}_0)]^2)$  for any fixed  $\alpha > d/2$ .

(b)  $\hat{c}_n(\hat{\alpha}_n, \beta) \xrightarrow{a.s.} c(\boldsymbol{\theta}_0)$  and  $\sqrt{n} \{ \hat{c}_n(\hat{\alpha}_n, \beta) - c(\boldsymbol{\theta}_0) \} \xrightarrow{\mathcal{L}} \mathcal{N}(0, 2[c(\boldsymbol{\theta}_0)]^2)$  for any fixed  $\beta > 0$ .

(c)  $\hat{c}_n(\hat{\boldsymbol{\theta}}_n) \xrightarrow{a.s.} c(\boldsymbol{\theta}_0)$  and  $\sqrt{n} \{ \hat{c}_n(\hat{\boldsymbol{\theta}}_n) - c(\boldsymbol{\theta}_0) \} \xrightarrow{\mathcal{L}} \mathcal{N}(0, 2[c(\boldsymbol{\theta}_0)]^2)$ .

*Proof.* We define sequences,  $\hat{c}_n(\alpha, \beta_L)$ ,  $\hat{c}_n(\alpha, \beta_U)$ ,  $\hat{c}_n(\alpha_L, \beta)$ , and  $\hat{c}_n(\alpha_U, \beta)$ . It follows from Lemma 1 that  $\hat{c}_n(\alpha, \beta_L) \leq \hat{c}_n(\alpha, \hat{\beta}_n) \leq \hat{c}_n(\alpha, \beta_U)$  and  $\hat{c}_n(\alpha_U, \beta) \leq \hat{c}_n(\hat{\alpha}_n, \beta) \leq \hat{c}_n(\alpha_L, \beta)$ . Applying Theorem 6 yields the desired results for  $\hat{c}_n(\alpha, \hat{\beta}_n)$  and  $\hat{c}_n(\hat{\alpha}_n, \beta)$ . To show the result for  $\hat{c}_n(\hat{\boldsymbol{\theta}}_n) = \hat{c}_n(\hat{\alpha}_n, \hat{\beta}_n)$ , it suffices to show that  $\hat{c}_n(\alpha_U, \beta_L) \leq \hat{c}_n(\hat{\alpha}_n, \hat{\beta}_n) \leq \hat{c}_n(\alpha_L, \beta_U)$  according to Lemma 1. In fact, we have,  $\hat{c}_n(\alpha_U, \beta_L) \leq \hat{c}_n(\alpha_U, \hat{\beta}) \leq \hat{c}_n(\hat{\alpha}_n, \hat{\beta}_n)$  and  $\hat{c}_n(\hat{\alpha}_n, \hat{\beta}_n) \leq \hat{c}_n(\alpha_L, \hat{\beta}_n) \leq \hat{c}_n(\alpha_L, \beta_U)$ .  $\square$

The first two results of Theorem 7 imply that the microergodic parameter can be estimated consistently by either fixing the tail decay parameter  $\alpha$  or the scale parameter  $\beta$ . In practice, fixing either  $\alpha$  or  $\beta$  may be too restrictive for modeling spatial processes. For instance, the microergodic parameter in the Matérn class can be estimated consistently when its range parameter is fixed. However, using the maximum likelihood estimator by jointly maximizing the likelihood over the variance parameter and the range parameter dramatically improves the prediction efficiency in a finite sample case (Kaufman and Shaby, 2013). Similarly, we would also expect that the finite sample prediction performance can be improved by jointly maximizing the variance parameter  $\sigma^2$ , the tail decay parameter  $\alpha$ , and the scale parameter  $\beta$  for the new covariance class.

The third result of Theorem 7 establishes that the microergodic parameter can be consistently estimated by jointly maximizing the log-likelihood (11) over the parameters  $\alpha$  and  $\beta$ . However, the current result requires that  $\alpha$  has to be greater than half of the dimension of the study domain. This means that the new covariance function cannot decay too slowly in its tail in order to establish the consistency result for the maximum likelihood estimator of the microergodic parameter. Nevertheless, this result shows a significant improvement over existing asymptotic normality results for other types of long-range dependent covariance functions. For instance, it was shown by Bevilacqua and Faouzi (2019) that the microergodic parameter in the generalized Cauchy class can be estimated consistently under infill asymptotics. However, their results assume that the parameter that controls the tail behavior is fixed. This is similar to the first result of Theorem 7. Unlike

their results, a pleasing theoretical improvement in Theorem 7 is that the asymptotic results for the microergodic parameter  $c(\boldsymbol{\theta})$  can be obtained for the joint estimation of all three parameters, including the parameter that controls the decay of the tail.

### 3.3 Asymptotic Prediction Efficiency

This section is focused on prediction of Gaussian process at a new location  $\mathbf{s}_0 \notin \mathcal{D}_n$ . This problem has been studied extensively when an incorrect covariance model is used. Our focus here is to show the asymptotic efficiency and asymptotically correct estimation of prediction variance in the context of the new covariance class. Stein (1988) shows that both of these two properties hold when the Gaussian measure under a misspecified covariance model is equivalent to the Gaussian measure under the true covariance model. In the case of the new covariance class, Theorem 4 gives the conditions for equivalence of two Gaussian measures in the light of the microergodic parameter  $c(\boldsymbol{\theta}) = \sigma^2 \beta^{-\nu} \Gamma(\nu + \alpha) / \Gamma(\alpha)$ .

Under the new covariance model  $C(h; \nu, \alpha, \beta, \sigma^2)$ , we define the best linear unbiased predictor for  $Z(\mathbf{s}_0)$  to be

$$\hat{Z}_n(\boldsymbol{\theta}) = \mathbf{r}_n^\top(\boldsymbol{\theta}) \mathbf{R}_n^{-1}(\boldsymbol{\theta}) \mathbf{Z}_n, \quad (12)$$

where  $\mathbf{r}_n(\boldsymbol{\theta}) := [R(\|\mathbf{s}_0 - \mathbf{s}_i\|; \boldsymbol{\theta}, \nu)]_{i=1, \dots, n}$  is an  $n$ -dimensional vector. This predictor depends only on  $\alpha, \beta, \nu$ . It is a misunderstanding of asymptotic results that if one fixes  $\boldsymbol{\theta} = \boldsymbol{\theta}_1$ , the prediction will improve as  $n$  grows due to the way  $\hat{c}_n(\boldsymbol{\theta})$  converges. This fact was also pointed out for the Matérn class by Kaufman and Shaby (2013).

If the true covariance is  $C(h; \nu, \alpha_0, \beta_0, \sigma_0^2)$ , the mean squared error of the predictor in Equation (12) is given by

$$\text{Var}_{\nu, \boldsymbol{\theta}_0, \sigma_0^2} \{ \hat{Z}_n(\boldsymbol{\theta}) - Z(\mathbf{s}_0) \} = \sigma_0^2 \left\{ 1 - 2\mathbf{r}_n^\top(\boldsymbol{\theta}) \mathbf{R}_n^{-1}(\boldsymbol{\theta}) \mathbf{r}_n(\boldsymbol{\theta}_0) + \mathbf{r}_n^\top(\boldsymbol{\theta}) \mathbf{R}_n^{-1}(\boldsymbol{\theta}) \mathbf{R}_n(\boldsymbol{\theta}_0) \mathbf{R}_n^{-1}(\boldsymbol{\theta}) \mathbf{r}_n(\boldsymbol{\theta}_0) \right\}.$$

If  $\boldsymbol{\theta} = \boldsymbol{\theta}_0$ , i.e.,  $\alpha = \alpha_0$  and  $\beta = \beta_0$ , the above expression simplifies to

$$\text{Var}_{\nu, \boldsymbol{\theta}_0, \sigma_0^2} \{ \hat{Z}_n(\boldsymbol{\theta}_0) - Z(\mathbf{s}_0) \} = \sigma_0^2 \left\{ 1 - \mathbf{r}_n^\top(\boldsymbol{\theta}_0) \mathbf{R}_n^{-1}(\boldsymbol{\theta}_0) \mathbf{r}_n(\boldsymbol{\theta}_0) \right\}. \quad (13)$$

If the true model is  $\mathcal{M}(h; \nu, \phi, \sigma^2)$ , analogous expressions can be derived for  $\text{Var}_{\nu, \phi_0, \sigma_0^2} \{ \hat{Z}_n(\boldsymbol{\theta}) - Z(\mathbf{s}_0) \}$ .

Let  $f_i(\omega), i = 1, 2$  be two spectral densities associated with two probability measures  $\mathcal{P}_i$ . Stein (1993) shows that the condition (6) together with  $f_2(\omega) / f_1(\omega) \rightarrow 1$  as  $\omega \rightarrow \infty$  implies that the best linear predictor (BLP) under a misspecified probability measure  $\mathcal{P}_2$  is asymptotically equivalent to the BLP under the true measure  $\mathcal{P}_1$ . The following results are immediate.

**THEOREM 8.** *Suppose that  $\mathcal{P}_0, \mathcal{P}_1$  are two Gaussian probability measures defined by a zero mean Gaussian process with the new covariance class  $C(h; \nu, \alpha_i, \beta_i, \sigma_i^2)$  for  $i = 1, 2$  on  $\mathcal{D}$ . If  $\alpha_i > d/2$ , then it follows that*

(a) As  $n \rightarrow \infty$ ,

$$\frac{\text{Var}_{\nu, \boldsymbol{\theta}_0, \sigma_0^2} \{ \hat{Z}_n(\boldsymbol{\theta}_1) - Z(\mathbf{s}_0) \}}{\text{Var}_{\nu, \boldsymbol{\theta}_0, \sigma_0^2} \{ \hat{Z}_n(\boldsymbol{\theta}_0) - Z(\mathbf{s}_0) \}} \rightarrow 1.$$

(b) Moreover, if  $\sigma_0^2 \beta_0^{-\nu} \Gamma(\nu + \alpha_0) / \Gamma(\alpha_0) = \sigma_1^2 \beta_1^{-\nu} \Gamma(\nu + \alpha_1) / \Gamma(\alpha_1)$ , then as  $n \rightarrow \infty$ ,

$$\frac{\text{Var}_{\nu, \theta_1, \sigma_1^2} \{ \hat{Z}_n(\boldsymbol{\theta}_1) - Z(\mathbf{s}_0) \}}{\text{Var}_{\nu, \theta_0, \sigma_0^2} \{ \hat{Z}_n(\boldsymbol{\theta}_1) - Z(\mathbf{s}_0) \}} \rightarrow 1.$$

*Proof.* Let  $f_i(\omega)$  be the spectral density of the new covariance functions  $C(h; \nu, \alpha_i, \beta_i, \sigma_i^2)$  with  $i = 1, 2$ . Note that  $\lim_{\omega \rightarrow \infty} f_i(\omega) |\omega|^{2\nu+d}$  is finite. If the condition in Equation (9) is satisfied, then,

$$\lim_{\omega \rightarrow \infty} \frac{f_2(\omega)}{f_1(\omega)} = \lim_{\omega \rightarrow \infty} \frac{f_2(\omega) |\omega|^{2\nu+d}}{f_1(\omega) |\omega|^{2\nu+d}} = 1.$$

These two statements follow by applying Theorem 1 and Theorem 2 of Stein (1993).  $\square$

Part (a) of Theorem 8 implies that if the smoothness parameter of  $\nu$  is correctly specified, any values for  $\alpha$  and  $\beta$  will result in asymptotically efficient estimates. The condition  $\sigma_0^2 \beta_0^{-\nu} \Gamma(\nu + \alpha_0) / \Gamma(\alpha_0) = \sigma_1^2 \beta_1^{-\nu} \Gamma(\nu + \alpha_1) / \Gamma(\alpha_1)$  is not necessary for asymptotic efficiency, but it provides asymptotically correct estimate of the mean squared prediction error. The quantity  $\text{Var}_{\nu, \theta_1, \sigma_1^2} \{ \hat{Z}_n(\boldsymbol{\theta}_1) - Z(\mathbf{s}_0) \}$  is the mean squared prediction error (MSPE) for  $\hat{Z}_n(\boldsymbol{\theta}_1)$  under the model  $C(h; \nu, \alpha_1, \beta_1, \sigma_1^2)$ , while the quantity  $\text{Var}_{\nu, \theta_0, \sigma_0^2} \{ \hat{Z}_n(\boldsymbol{\theta}_1) - Z(\mathbf{s}_0) \}$  is the true MSPE for  $\hat{Z}_n(\boldsymbol{\theta}_1)$  under the true model  $C(h; \nu, \alpha_0, \beta_0, \sigma_0^2)$ . In practice, it is common to estimate model parameters and then prediction is made by plugging in these estimates into Equations (12) and (13). Next, we show the same convergence results if  $\boldsymbol{\theta}$  is fixed at  $\boldsymbol{\theta}_1$ , but  $\sigma^2$  is estimated via maximum likelihood method. This is one extension of Part (b) of Theorem 8, with its proof given in Section S.8 of the Supplementary Material.

**COROLLARY 2.** Suppose that  $\mathcal{P}_0, \mathcal{P}_1$  are two Gaussian probability measures defined by a zero mean Gaussian process with the new covariance class  $C(h; \nu, \alpha_i, \beta_i, \sigma_i^2)$  for  $i = 1, 2$  on  $\mathcal{D}$ . Let  $\hat{\sigma}_n^2 = \mathbf{Z}_n^\top \mathbf{R}_n^{-1}(\boldsymbol{\theta}_1) \mathbf{Z}_n / n$ . If  $\alpha_i > d/2$ , then it follows that almost surely under  $\mathcal{P}_0$ , as  $n \rightarrow \infty$ ,

$$\frac{\text{Var}_{\nu, \theta_1, \hat{\sigma}_n^2} \{ \hat{Z}_n(\boldsymbol{\theta}_1) - Z(\mathbf{s}_0) \}}{\text{Var}_{\nu, \theta_0, \sigma_0^2} \{ \hat{Z}_n(\boldsymbol{\theta}_1) - Z(\mathbf{s}_0) \}} \rightarrow 1.$$

One can conjecture that the result in Corollary 2 still holds if  $\boldsymbol{\theta}_1$  is replaced by its maximum likelihood estimator, but its proof seems elusive. Theorem 8 and Corollary 2 demonstrate the asymptotic prediction efficiency for the new covariance class. The following results are established to show the asymptotic efficiency of the best linear predictor under the new covariance class when the true Gaussian measure is generated by a zero-mean Gaussian process under the Matérn class.

**THEOREM 9.** Let  $\mathcal{P}_0$  be the Gaussian probability measure defined by a zero mean Gaussian process with the Matérn covariance class  $\mathcal{M}(h; \nu, \phi, \sigma_0^2)$  and  $\mathcal{P}_1$  be the Gaussian probability measure defined by a zero mean Gaussian process with the new covariance class  $C(h; \nu, \alpha, \beta, \sigma_1^2)$  on  $\mathcal{D}$ . If  $\alpha > d/2$  and the condition in Equation (10) is satisfied, then it follows that under the Gaussian measure  $\mathcal{P}_0$ , as  $n \rightarrow \infty$ ,

$$\frac{\text{Var}_{\nu, \alpha, \beta, \sigma_1^2} \{ \hat{Z}_n(\alpha, \beta, \nu) - Z(\mathbf{s}_0) \}}{\text{Var}_{\nu, \phi, \sigma_0^2} \{ \hat{Z}_n(\phi, \nu) - Z(\mathbf{s}_0) \}} \rightarrow 1,$$

for any fixed  $\alpha > d/2$  and  $\beta > 0$ .

*Proof.* Let  $f_0(\omega)$  be the spectral density of the Matérn covariance function  $\mathcal{M}(h; \nu, \phi, \sigma_0^2)$  and  $f_1(\omega)$  be the spectral density of the covariance function  $C(h; \nu, \alpha, \beta, \sigma_1^2)$ . Notice that the spectral density of the Matérn covariance satisfies the condition (6). It suffices to show that  $\lim_{\omega \rightarrow \infty} f_1(\omega)/f_0(\omega) = 1$ . Let  $k_0 = \sigma_0^2 \phi^{-2\nu}$  and  $k_1 = \sigma_1^2 (\beta/2)^{-\nu} \Gamma(\nu + \alpha) / \Gamma(\alpha)$ . If  $k_0 = k_1$ , it follows that

$$\lim_{\omega \rightarrow \infty} \frac{f_1(\omega)}{f_0(\omega)} = \lim_{\omega \rightarrow \infty} \frac{f_1(\omega) |\omega|^{2\nu+d}}{f_0(\omega) |\omega|^{2\nu+d}} = \lim_{\omega \rightarrow \infty} \frac{k_1}{k_0} (2\nu \phi^{-2} \omega^{-2} + 1)^{\nu+d/2} = k_1/k_0 = 1.$$

Thus, the covariance function  $C(h; \nu, \alpha, \beta, \sigma_1^2)$  yields an asymptotically equivalent BLP as the Matérn covariance  $\mathcal{M}(h; \nu, \phi, \sigma_0^2)$ .  $\square$

A key consequence of Theorem 9 is that when a true Gaussian process is generated by the Matérn covariance model, the new covariance model of Equation (3) can yield an asymptotically equivalent BLP. However, when the true Gaussian process is generated by the new covariance model with  $\alpha \in (0, d/2]$ , there is no situation where the Matérn covariance model satisfies the same property. The practical implication is when the true model is generated from the Matérn class, the predictive performance under the new covariance class is indistinguishable from that under the Matérn class as the number of observations gets larger in a fixed domain. However, when the true model is generated from the new covariance class, the predictive performance under the Matérn class is expected to be worse than that under the new covariance class, since the new covariance class with  $\alpha > d/2$  can yield asymptotically equivalent BLP as the Matérn class while the Matérn class cannot yield asymptotically equivalent BLP as the new covariance class with  $\alpha \in (0, d/2]$ . Theorem 9 provides a strong argument in favor of the proposed covariance class when a choice needs to be made between the new covariance class and the Matérn class in situations where there is little or no information on the underlying true covariance structure.

## 4 Numerical Illustrations

In this section, we use simulated examples to study the properties of the new covariance class and compare with alternative covariance models. In Section 4.1, we compare the new covariance model with the other two covariance models: the Matérn class and the generalized Cauchy class. The predictive performance is evaluated based on root mean-squared prediction errors (RMSPE), coverage probability of the 95% percentile confidence intervals (CVG), and the average length of the predictive confidence intervals (ALCI) at held-out locations. In Section 4.2, we illustrate the asymptotic normality of the MLE for the microergodic parameter with sample sizes  $n = 4000, 5000, 6000$  under different parameter settings. The statistical analysis was performed with the statistical software R (R Core Team, 2018) and the R package `ggplot2` (Wickham, 2016).

### 4.1 Examples to Illustrate the Predictive Performance

The goal of this section is to study the finite sample predictive performance under the new covariance model. Specifically, we consider three different cases, where the true covariance model

is specified as the Matérn covariance (Case 1), the new covariance (Case 2) and the generalized Cauchy (GC) covariance (Case 3), respectively. The Matérn class is very flexible near origin and has an exponentially decaying tail, the new covariance class is also very flexible near origin but has a polynomially decaying tail, and the GC class is either non-differentiable or infinitely differentiable and has a polynomially decaying tail. The GC covariance has the form  $C(h) = \sigma^2 \{1 + (h/\phi)^\delta\}^{-\lambda/\delta}$ , where  $\sigma^2 > 0$  is the variance parameter,  $\phi > 0$  is the range parameter,  $\lambda \in (0, d]$  is the parameter controlling the degree of polynomial decay, and  $\delta \in (0, 2]$  is the smoothness parameter. When  $\delta \in (0, 2)$ , the corresponding process realizations will be non-differentiable. When  $\delta = 2$ , the process realizations will be infinitely differentiable. For each case, predictive performance is compared at held-out locations with estimated covariance structures.

We simulate data in the square domain  $\mathcal{D} = [0, 2000] \times [0, 2000]$  from mean zero Gaussian processes with three different covariance function models: the Matérn covariance (Case 1), the new covariance (Case 2) and the GC covariance (Case 3) for a variety of settings. We simulate  $n = 500, 1000, 2000$  data points via maximin Latin hypercube design (Stein, 1987) for parameter estimation and evaluate predictive performance at 10-by-10 regular grid points in  $\mathcal{D}$ . We fix the variance parameter at 1 and consider moderate spatial dependence with effective range (ER) at 200 and 500 for the underlying true covariances. For each of these simulation settings, we use 30 different random number seeds to generate the realizations. We always choose the same smoothness parameter for the Matérn class and the new covariance class. For the GC covariance, we fix its smoothness parameter to be  $\delta = \min\{2\nu, d\}$ , since the Gaussian measure with the Matérn class is equivalent to that with the GC class under certain conditions when the smoothness parameter of the GC class is twice the smoothness parameter of the Matérn class (Bevilacqua and Faouzi, 2019). However, the smoothness parameter  $\delta$  in the GC class cannot be greater than 2, otherwise the GC class is no longer a valid covariance function. For numerical stability reason, the parameter  $\alpha$  in the new covariance class is constrained in the interval  $[10^{-5}, 6]$  when we perform the maximum likelihood estimation. When  $\alpha$  is too small, numerical evaluation of the new covariance may be unstable. When  $\alpha$  is too large, numerical evaluation of the new covariance function is also unstable because of difficulties in computing the confluent hypergeometric function. Notice that  $\alpha = 10^{-5}$  corresponds to extremely slow decay of the tail and  $\alpha = 6$  corresponds to very fast decaying tail.

In Case 1, we simulate Gaussian process realizations from the Matérn model with smoothness parameter  $\nu$  fixed at 0.5 and 2.5 and effective range at 200 and 500. The parameters in each covariance model are estimated based on profile likelihood as described in Section 3.2. Figure 4 shows the estimated covariance structures and summary of prediction results. Regardless of the smoothness behavior and strength of dependence in the underlying true process, there is no clear difference between the new covariance class and the Matérn class in terms of estimated covariance structures and prediction performance. In contrast, the estimated GC covariance structure only performs as accurately as the Matérn class when  $\nu = 0.5$ . When the process realizations are twice differentiable ( $\nu = 2.5$ ), as expected, the GC class cannot mimic such behavior, and hence, yields worse estimates of the covariance structures and prediction results compared to both the Matérn class and the new covariance class. The new covariance is able to capture the true covariance structure although it is not as accurate as the estimated Matérn covariance. In terms of RMSPE, there is no clear difference between the estimates under the new covariance class and the estimates under the Matérn class. However, the CVG and ALCI based on the new covariance class

are slightly larger than those based on the estimated Matérn covariance.

In Case 2, we simulate Gaussian process realizations from the new covariance model with smoothness parameter  $\nu$  fixed at 0.5 and 2.5, tail decay parameter fixed at 0.5, and effective range fixed at 200 and 500. Figure 5 shows the estimated covariance structures and summary of prediction results. As expected, when the underlying true process is simulated from a long-memory process, the Matérn class cannot be expected to capture such behavior. The prediction results also indicate that the Matérn class performs much worse than the other two covariance models. When the underlying true process is not differentiable ( $\nu = 0.5$ ), there is no clear difference between the estimates under the GC covariance structure and the estimates under the new covariance structure. However, when the underlying true process is twice differentiable ( $\nu = 2.5$ ), it is obvious that the estimates under the GC covariance structure is not as accurate as the estimates under the new covariance structure. This makes sense because the GC class is either non-differentiable or infinitely differentiable. In terms of prediction performance, the new covariance class performs better than the GC class in terms of coverage probability.

In Case 3, we simulate Gaussian process realizations from the GC class with the smoothness parameter  $\delta = 1$  and  $\lambda = 1$  under ER=200 and 500. The corresponding process is non-differentiable and corresponds to the smoothness parameter  $\nu = 0.5$  in both the Matérn class and the new covariance class. The parameter  $\lambda$  in the GC class is fixed at 1 so that it corresponds to the tail parameter  $\alpha = 0.5$  in the new covariance class. We did not consider Gaussian process realizations that are infinitely differentiable, since such process realizations are unrealistic for environmental processes. Figure 6 shows the estimated covariance structures and prediction results. As expected, the Matérn class performs much worse than the new covariance class and the GC class for the same reason as in Case 2. Between the new covariance class and the GC class, no difference is seen in terms of estimated covariance structures and predictive performances. This is not surprising, since the new covariance class has a tail decay parameter  $\alpha$  that is able to capture the tail behavior in the GC class.

The results in these three cases are based  $n = 2000$  observations. In Section S.1 of the Supplementary Material, we provide results on exactly the same simulation settings with  $n = 500$  and 1000. Similar conclusions can be drawn there. In addition, we also investigate the predictive performance when the covariance of the underlying true process is a product of individual covariance functions; see Section S.2 of the Supplementary Material. In all these simulation examples, we found that the new covariance class to be quite flexible in terms of capturing both the smoothness and the tail behavior. No matter which covariance structure (the Matérn class or the GC class) the true underlying process is generated from, the new covariance class is able to capture the underlying true covariance structure with satisfactory performance. In contrast, the Matérn class is not able to capture the underlying true covariance structure with long-range dependence and the GC class is not able to capture the underlying true covariance structure with different degrees of smoothness behavior.

## 4.2 Examples to Illustrate Asymptotic Normality

As shown in Section 3.2, each individual parameter in the new covariance model cannot be estimated consistently, however, the microergodic parameter can be estimated consistently.

To study the finite sample performance of the asymptotic properties of MLE for the microer-

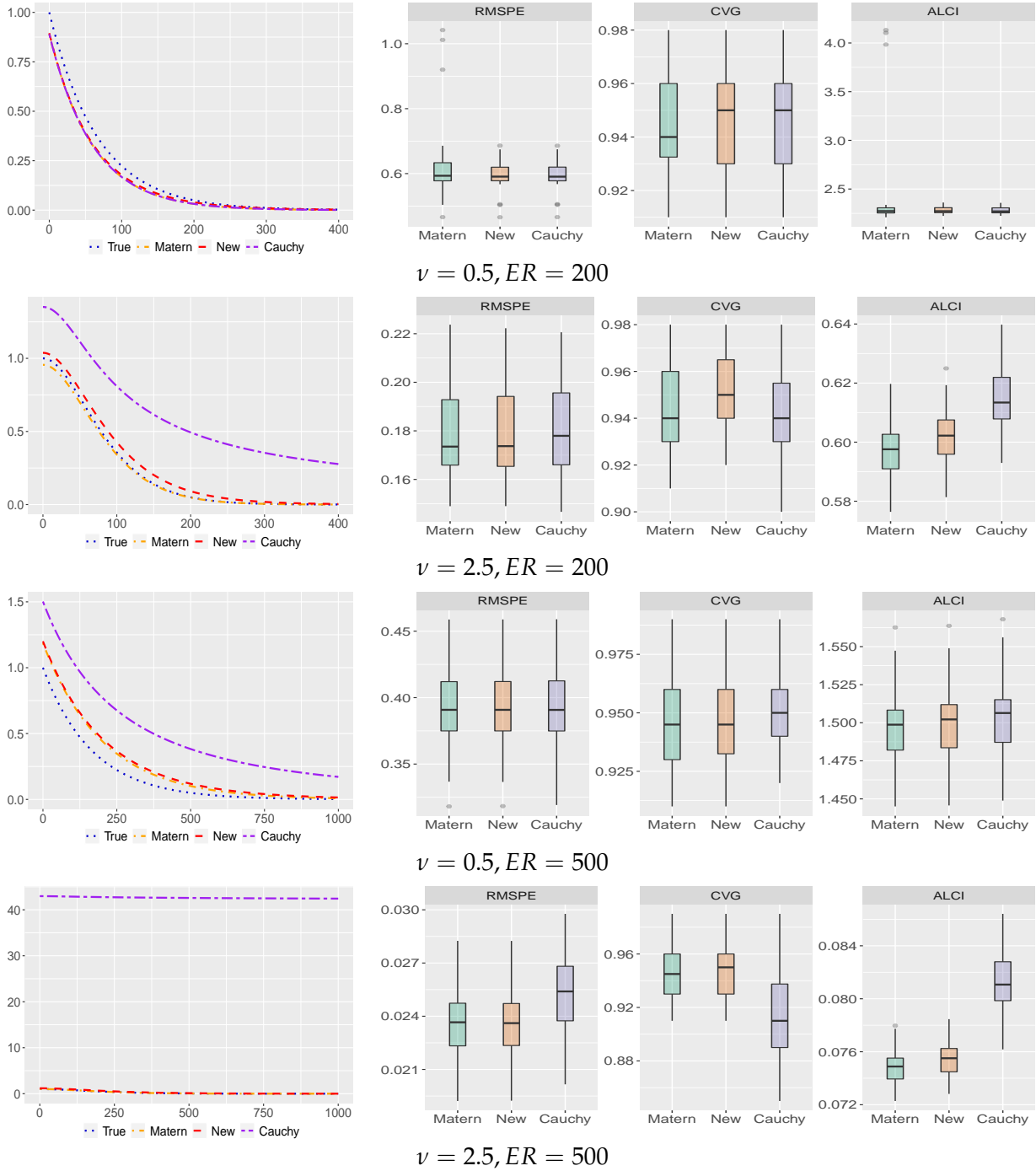


**Fig. 4.** Case 1: Comparison of predictive performance and estimated covariance structures when the true covariance is the Matérn class with 2000 observations. The predictive performance is evaluated at 10-by-10 regular grids in the square domain. These figures summarize the predictive measures based on RMSPE, CVG and ALCI under 30 simulated realizations.

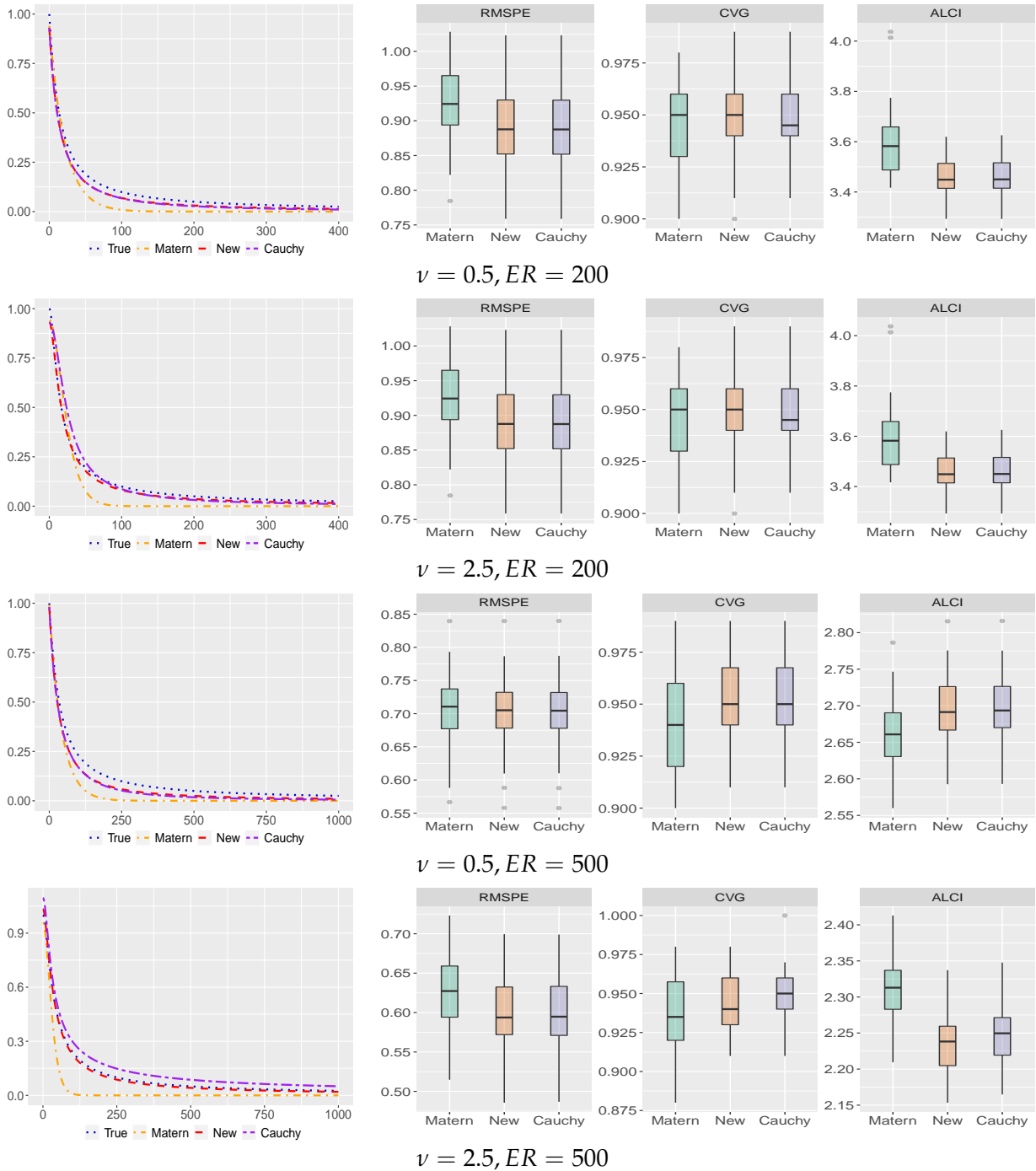


**Fig. 5.** Case 2: Comparison of predictive performance and estimated covariance structures when the true covariance is the new covariance class with 2000 observations. The predictive performance is evaluated at 10-by-10 regular grids in the square domain. These figures summarize the predictive measures based on RMSPE, CVG and ALCI under 30 simulated realizations.

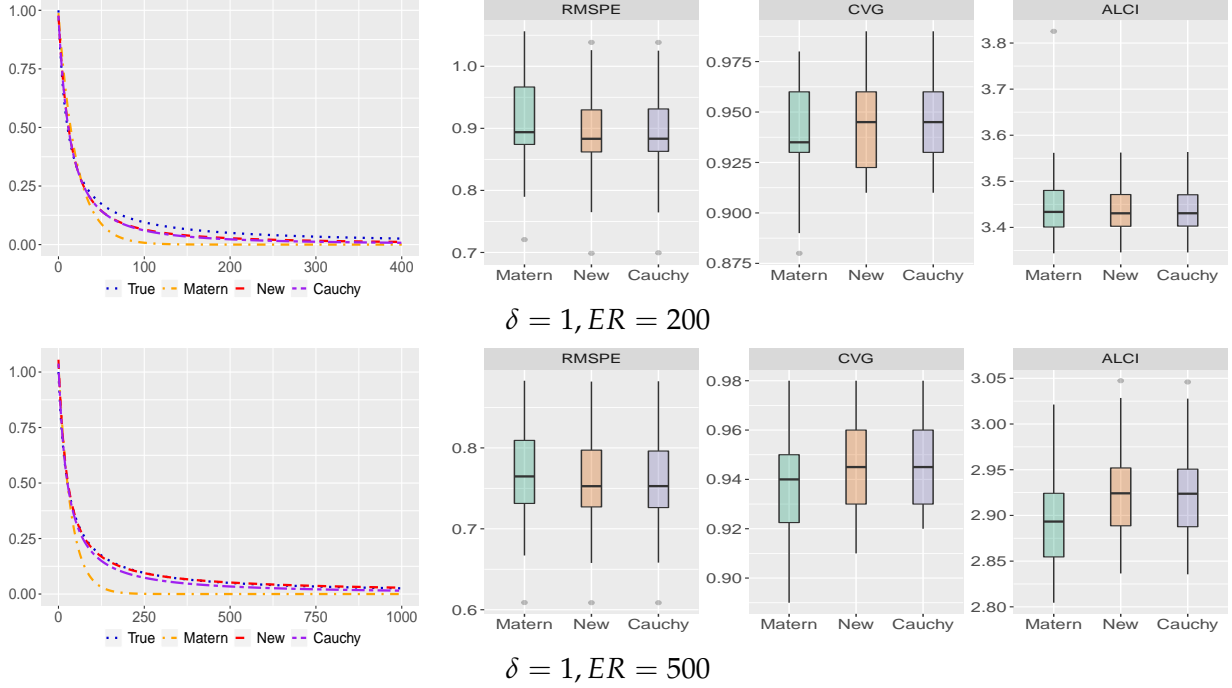


**Fig. 6.** Case 3: Comparison of predictive performance and estimated covariance structures when the true covariance is the GC class with 2000 observations. The predictive performance is evaluated at 10-by-10 regular grids in the square domain. These figures summarize the predictive measures based on RMSPE, CVG and ALCI under 30 simulated realizations.

godic parameter, we simulate 1000 realizations from a zero-mean Gaussian process with the new covariance class over 100-by-100 regular grid in the unit domain  $\mathcal{D} = [0, 1] \times [0, 1]$ . As there are no clear guidelines to pick the sample sizes such that the finite sample performances can appropriately reflect the asymptotic results, we randomly select  $n = 4000, 5000, 6000$  locations from these 10,000 grid points. The variance parameter is fixed at 1 for all realizations. We consider two different values for the smoothness parameter  $\nu$  at 0.5 and 1.5, three different values for the tail decay parameter  $\alpha$  at 0.5, 2 and 5. The scale parameter  $\beta$  is chosen such that the effective range is 0.6 or 0.9. Although all the theoretical results in Section 3 are valid for  $\alpha > d/2$ , we also run the simulation setting with  $\alpha = 0.5$  to see whether there is any interesting numerical results compared to cases where  $\alpha > d/2$ .

Let  $C(h; \nu, \alpha_0, \beta_0, \sigma_0^2)$  be the true covariance. We use  $\hat{c}_n(\boldsymbol{\theta})$  to denote the maximum likelihood estimator of the microergodic parameter  $c(\boldsymbol{\theta}_0) = \sigma_0^2 \beta_0^{-\nu} \Gamma(\nu + \alpha_0) / \Gamma(\alpha_0)$  for any  $\boldsymbol{\theta}$ . Then the 95% confidence interval for  $c(\boldsymbol{\theta}_0)$  is given by  $\hat{c}_n(\boldsymbol{\theta}) \pm 1.96 \sqrt{2\hat{c}_n(\boldsymbol{\theta})^2/n}$ . Theorems 6 and 7 show that this interval is asymptotically valid when  $n$  is large and  $\alpha > d/2$  for (1) arbitrarily fixed  $\boldsymbol{\theta}$ , (2)  $\boldsymbol{\theta} = (\alpha, \hat{\beta}_n)$ , (3)  $\boldsymbol{\theta} = (\hat{\alpha}_n, \beta)$  and (4)  $\boldsymbol{\theta} = (\hat{\alpha}_n, \hat{\beta}_n)$ . In this simulation study, we primarily focus on the finite sample performance of  $\hat{c}_n(\boldsymbol{\theta})$ , where  $\boldsymbol{\theta} = (\alpha_0, 0.5\beta_0)$ ,  $\boldsymbol{\theta} = (\alpha_0, \beta_0)$ ,  $\boldsymbol{\theta} = (\alpha_0, 2\beta_0)$ ,  $\boldsymbol{\theta} = (\alpha_0, \hat{\beta}_n)$ , and  $\boldsymbol{\theta} = (\hat{\alpha}_n, \hat{\beta}_n)$ . Exhaustive simulations with all other settings of  $\boldsymbol{\theta}$  is considered future work. Let

$$\zeta := \frac{\sqrt{n}\{\hat{c}_n(\boldsymbol{\theta}) - c(\boldsymbol{\theta}_0)\}}{\sqrt{2c(\boldsymbol{\theta}_0)}}.$$

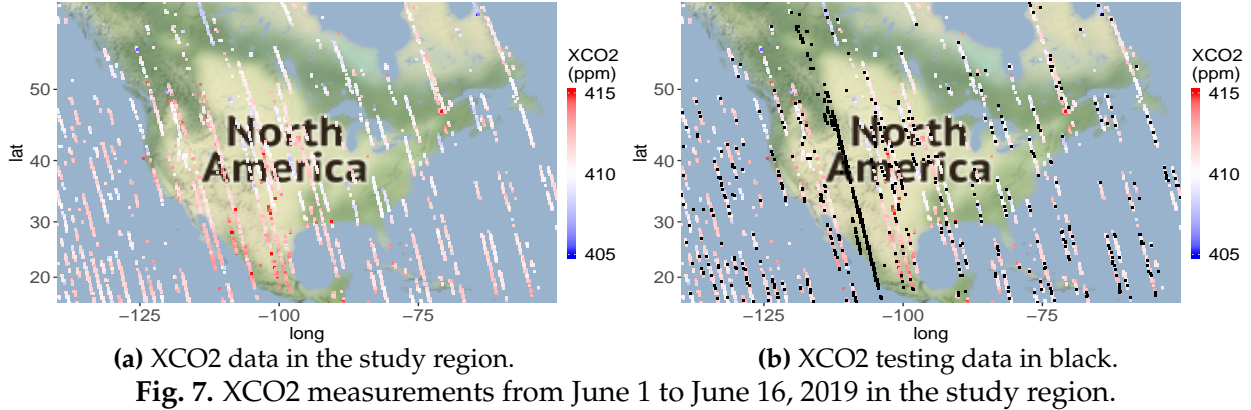
Then  $\zeta$  should asymptotically follow the standard normal distribution. Based on these 1000 realizations, we compute the empirical coverage probability of the 95% percentile confidence interval, bias and root-mean-square error (RMSE) for  $c(\theta_0)$  and compare the quantiles of  $\zeta$  with the standard normal quantiles.

The results are reported in Table S.1, Table S.2 and Table S.3 of the Supplementary Material. They can be summarized as follows. When the true parameters are used, i.e.,  $\theta = \theta_0$ , as expected, the sampling distribution of  $\hat{c}_n(\theta_0)$  gives the best normal approximation and converges to the asymptotic distribution in Theorem 6 when  $n$  increases. The sampling distribution of  $\hat{c}_n(\theta)$  can be highly biased and approach to the truth can be very slow with increase in  $n$ . Fixing  $\beta$  at a larger value gives better empirical results than fixing  $\beta$  at a small value. When the scale parameter is chosen to be its maximum likelihood estimator, i.e.,  $\beta = \hat{\beta}_n$ , the sampling distribution of  $\hat{c}_n(\alpha, \hat{\beta}_n)$  converges to the asymptotic distribution given in Theorem 7 as  $n$  increases. When  $\alpha$  is small, e.g.,  $\alpha = 0.5$ , the sampling distributions of  $\hat{c}_n(\theta)$ , with  $(\alpha_0, 0.5\beta_0)$ ,  $(\alpha_0, 2\beta_0)$ ,  $(\alpha_0, \hat{\beta}_n)$  and  $(\hat{\alpha}_n, \hat{\beta}_n)$  substituted for  $\theta$ , has noticeable biases. As the tail decay parameter or the effective range increases, the sampling distributions of  $\hat{c}_n(\theta)$  have smaller biases. As  $\nu$  becomes smaller, the sampling distributions of  $\hat{c}_n(\theta)$  approaches the truth better with increase in  $n$ . When  $\nu = 0.5$  and  $\alpha \in \{2, 5\}$ , these sampling distributions have negligible biases as  $n$  increases. When both  $\alpha$  and  $\beta$  are substituted by their maximum likelihood estimator, the sampling distribution of  $\hat{c}_n(\theta)$  has smaller bias and gives better approximation to the true asymptotic distribution given in Theorem 7 as  $n$  increases for  $\alpha > d/2 = 1$ .

When  $\alpha$  is fixed at its true value and  $\beta$  is estimated by maximum likelihood method, the MLE of the microergodic parameter,  $\hat{c}_n(\alpha, \hat{\beta}_n)$ , gives better finite sample performance than the cases where  $\beta$  is misspecified. When both  $\alpha$  and  $\beta$  are estimated by maximum likelihood method, the MLE of the microergodic parameter,  $\hat{c}_n(\hat{\alpha}_n, \hat{\beta}_n)$ , also gives better finite sample performance than the cases where  $\beta$  is misspecified and  $\alpha$  is fixed at its true value. One would also expect that this is true when either  $\alpha$  or  $\beta$  is misspecified at incorrect values. In general, the MLE of the microergodic parameter has better finite sampler performance than those with any individual parameter fixed at an incorrect value in the microergodic parameter. Theorem 7 requires  $\alpha > d/2$  in order to derive asymptotic results for  $\hat{c}_n(\hat{\alpha}_n, \hat{\beta}_n)$ . However, it is interesting to observe from these simulation results that  $\hat{c}_n(\theta)$  seems to converge to a normal distribution even when  $\alpha < d/2$ , i.e., when  $\alpha = 0.5$ . It is an open problem to determine the exact distribution that the maximum likelihood estimator  $\hat{c}_n(\hat{\alpha}_n, \hat{\beta}_n)$  of the microergodic parameter converges to asymptotically when  $\alpha$  and  $\beta$  are substituted with their maximum likelihood estimators for true  $\alpha_0 \in (0, d/2]$ .

## 5 Application to the OCO-2 Data

In this section, the proposed new covariance class is used to model spatial data collected from NASA's Orbiting Carbon Observatory-2 (OCO-2) satellite and comparisons are made in kriging performances with alternative covariances. The OCO-2 satellite is NASA's first dedicated remote sensing earth satellite to study atmospheric carbon dioxide from space with the primary objective to estimate the global geographic distribution of CO<sub>2</sub> sources and sinks at Earth's surface; see Cressie (2017); Wunch et al. (2011) for detailed discussions. The OCO-2 satellite carries three high-resolution grating spectrometers designed to measure the near-infrared absorption of re-



flected sunlight by carbon dioxide and molecular oxygen and orbits over a 16-day repeat cycle. In this application, we consider NASA’s Level 3 data product of the XCO2 at  $0.25^\circ \times 0.25^\circ$  spatial resolution over one repeat cycle from June 01 to June 16, 2019. These gridded data were processed based on Level 2 data product by the OCO-2 project at the Jet Propulsion Laboratory, California Technology, and obtained from the OCO-2 data archive maintained at the NASA Goddard Earth Science Data and Information Services Center. They can be downloaded at <https://co2.jpl.nasa.gov/#mission=OCO-2>.

This Level 3 data product consists of 43,698 measurements. We focus on the study region that covers the entire United States with longitudes between 140W and 50W and latitudes between 15N and 60N. This region includes 3,682 measurements; see panel (a) of Figure 7. These data points are very sparse in space. As the OCO-2 satellite has swath width 10.6 kilometers, large missing gaps can be observed between swaths. Predicting the underlying geophysical process based on data with such patterns requires the statistical model not only to interpolate in space (prediction near observed locations) but also to extrapolate in space (prediction away from observed locations).

Given the data  $\mathbf{Z} := (Z(\mathbf{s}_1), \dots, Z(\mathbf{s}_n))^T$ , we assume a typical spatial process model:

$$Z(\mathbf{s}) = Y(\mathbf{s}) + \epsilon(\mathbf{s}), \quad \mathbf{s} \in \mathcal{D},$$

where  $Y(\cdot)$  is assumed to be a Gaussian process with mean function  $\mu(\cdot)$  and covariance function  $C(\cdot, \cdot)$ . The term  $\epsilon(\cdot)$  is assumed to be a spatial white-noise process accounting for the nugget effect with  $\text{var}(\epsilon(\mathbf{s})) = \tau^2 > 0$ . The goal of this analysis is to predict the process  $Y(\mathbf{s}_0)$  for any  $\mathbf{s}_0 \in \mathcal{D}$  based on the data  $\mathbf{Z}$ . Exploratory analysis indicates no clear trend, so we assume a constant trend for the mean function  $\mu(\mathbf{s}) = b$ . For the covariance function  $C(\cdot, \cdot)$ , we assume the new covariance function model with parameters  $\{\sigma^2, \alpha, \beta, \nu\}$ , where the smoothness parameter  $\nu$  is fixed at 0.5 and 1.5, which indicates the resulting process is non-differentiable or once differentiable, respectively.

To evaluate the performance of the new covariance function model, we perform cross-validation and make comparisons with the Matérn class. The testing dataset consists of (1) a complete longitude band across the United States, which will be referred to as missing by design (MBD) and (2) randomly selected 15% of remaining XCO2 measurements, which will be referred to as missing at random (MAR). Panel (b) of Figure 7 highlights these testing data with black grid points. This dataset is used for evaluating out-of-sample predictive performance in an interpolative setting and an extrapolative setting. The remaining data points are used for parameter estimation under

the Matérn covariance model and the new covariance model. The parameters are estimated based on the restricted maximum likelihood (Harville, 1974). Table 1 shows the predictive measures and estimated nugget parameters. The new covariance model with the smoothness parameter  $\nu = 0.5$  yields the smallest estimated nugget parameter among all the models. This suggests that the new covariance model with  $\nu = 0.5$  best captures the spatial dependence structure among all the models. In an interpolative setting, the Matérn covariance model yields slightly smaller RMSPE and ALCI over randomly selected locations than the new covariance model, which indicates that the Matérn covariance model has slightly better short-range prediction skill than the new covariance model. The empirical coverage probability is closer to the nominal value of 0.95 under the Matérn covariance model. In contrast, in an extrapolative setting, the new covariance model yields much smaller RMSPE and ALCI than the Matérn covariance model with indistinguishable empirical coverage probabilities, which indicates that the new covariance model has a better long-range prediction skill than the Matérn covariance model. These prediction results are not surprising, since the Matérn class can only model short-range dependence while the new covariance class can offer considerable benefits in long-range prediction. The difference in short-range prediction performances between the new covariance class and the Matérn class is very small, in part because the new covariance class can yield asymptotically equivalent best linear predictors as the Matérn class under conditions established in Theorem 9. Notice that the empirical coverage probabilities under all the models are less than the nominal coverage probability 0.95, this is partly because uncertainties due to parameter estimation are not accounted for in the predictive distribution. A fully Bayesian analysis may remedy this issue.

For other model parameters shown in Table S.4 of the Supplementary Material, we notice that the estimates of the regression parameters under the two different covariance models are the same. As expected, the estimated variance parameter (partial sill) is larger under the new covariance class than the one estimated under the Matérn class. Perhaps the most interesting parameter is the tail decay parameter in the new covariance class, which is estimated to be around 0.38. This clearly indicates that the underlying true process has a long-range dependence structure. As Gneiting (2013) points out, the Matérn class is positive definite on sphere only if  $\nu \leq 0.5$  with great circle distance. To avoid this technical difficulty, we use chordal distance for modeling spatial data on sphere when  $\nu > 0.5$ , since Yadrenko (1983) points out that chordal distance can guarantee the positive definiteness of a covariance function on  $\mathbb{S}^d \times \mathbb{S}^d$  when the original covariance function is positive definite on  $\mathbb{R}^{d+1} \times \mathbb{R}^{d+1}$ .

**Table 1.** Cross-validation results on the XCO2 data based on the Matérn covariance model and the new covariance model. The measures in the first coordinate correspond to those based on MAR locations, and the measures in the second coordinate correspond to those based on MBD locations.

	Matérn class		New covariance class	
	$\nu = 0.5$	$\nu = 1.5$	$\nu = 0.5$	$\nu = 1.5$
RMSPE	(0.672, 1.478)	(0.675, 1.599)	(0.676, 1.263)	(0.735, 1.227)
CVG(95%)	(0.952, 0.929)	(0.952, 0.951)	(0.944, 0.921)	(0.878, 0.937)
ALCI(95%)	(2.533, 5.095)	(2.536, 5.044)	(2.543, 4.722)	(2.098, 4.855)
$\tau^2$ (nugget)	0.0642	0.2215	0.0038	0.1478

Next, we predict the process  $Y(\cdot)$  at  $0.25^\circ \times 0.25^\circ$  grid in the study region. The parameters are

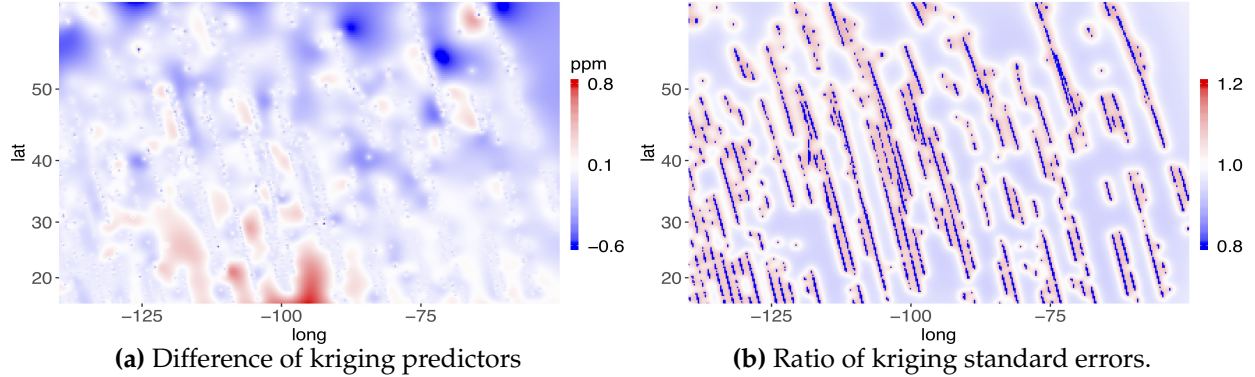


**Fig. 8.** Comparison of kriging predictions under the Matérn class and the new covariance class. The left panel shows the difference between kriging predictors under the new covariance class and those under the Matérn class. The right panel shows the ratio of kriging standard errors under the new covariance class to those under the Matérn class.

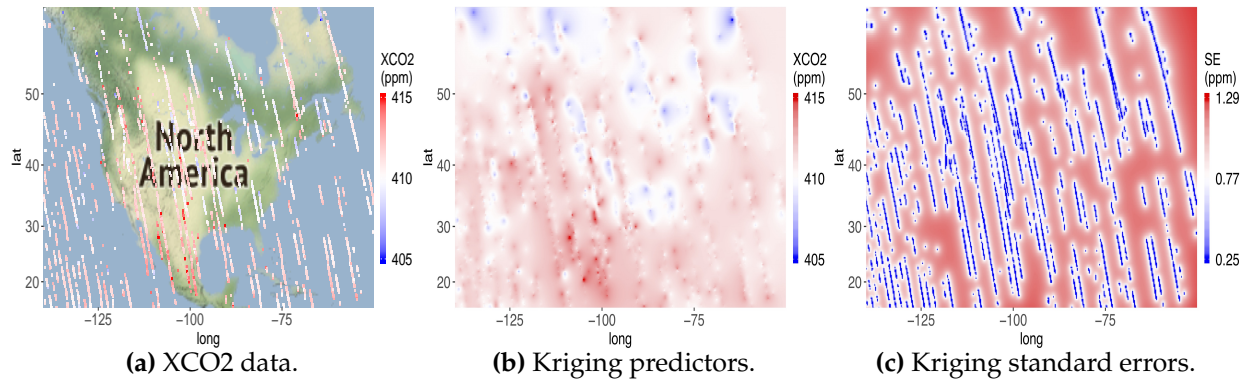


**Fig. 9.** XCO2 data and kriging predictions based on the new covariance model.

estimated based on all the data points under the new covariance class and the Matérn class with the smoothness parameter fixed at 0.5. In Figure 8, we observe that the optimal kriging predictors over these grid points under the new covariance model generally yield smaller values than those under the Matérn covariance function model in large missing gaps except for certain regions such as the Gulf of Mexico. More importantly, we also observe that the new covariance model yields 10% to 20% smaller kriging standard errors than the Matérn covariance model in the observed spatial locations and contiguous missing regions. This indicates that the new covariance model has an advantage over the Matérn covariance in terms of in-sample prediction skills and in an extrapolative setting (such as large missing gaps). Prediction in an interpolative setting (such as locations near the observed locations) shows that the new covariance yields slightly larger (no more than 2%) kriging standard errors compared to the Matérn covariance class. Finally, we show in Figure 9 the optimal kriging predictors and associated kriging standard errors at  $0.25^\circ \times 0.25^\circ$  grid in the study region. These kriging maps help create a complete NASA Level 3 data product with associated uncertainties quantified in a statistically optimal way.

## 6 Discussion

This paper introduces a new class of covariance functions that can allow precise and simultaneous control of the origin and tail behaviors. Our approach in constructing the new covariance class is to mix over the range parameter of the Matérn class. As expected, the origin behavior of this new covariance class is as flexible as the Matérn class. The high-frequency behavior of the new covariance class is also similar to that of the Matérn class, since they differ by a slowly varying function up to a multiplicative constant when the new covariance function does not decay too slow, i.e.,  $\alpha > d/2$ . Unlike the Matérn class, however, this new covariance class has a polynomially decaying tail, which allows for modeling long-memory stochastic processes. Conditions for equivalence of two Gaussian measures based on this new covariance class are established. We derive the conditions on the asymptotic efficiency of kriging predictors based on an increasing number of observations in a bounded region when the new covariance function is misspecified. We also show that the new covariance function can yield an asymptotically efficient kriging predictor under the infill asymptotics framework when the true covariance belongs to the Matérn class. It is worth noting that the covariance function itself is valid and can allow any degrees of decaying tail with  $\alpha > 0$ , while the theoretical results are proven for  $\alpha > d/2$ . Investigation of similar theoretical results is elusive for the case  $\alpha \in (0, d/2]$ , because Bochner's theorem cannot be applied directly. Extensive simulation results show that when the underlying true process is generated from either the Matérn covariance or the GC covariance, the new covariance function can yield as good a predictive performance as the underlying true covariance model. In the real data analysis, we also highlight the advantages of the new covariance function when used for prediction in an extrapolative setting. This feature is practically important for spatial modeling with large missing patterns.

This new covariance class not only plays an important role in spatial statistics, but also is of particular interest in UQ. In the UQ community, a covariance function that is of a product form (e.g., Sacks et al., 1989; Santner et al., 2018) has been widely used to model dependence structures for computer model output to allow for different physical interpretations in each input dimension. The product form of this new covariance function can not only control the smoothness of the process realizations in each direction but also allow long-range dependence in each direction. We give a simulation example in Section S.2 of the Supplementary Material to illustrate the advantage of the product form of the new covariance function. Predicting real-world processes often relies on computer models whose output can have different smoothness properties and can be insensitive to certain inputs. This new covariance class can not only allow flexible control over the smoothness of the physical process of interest, but also allow near constant behavior along these inert inputs. Most often, predicting the real-world process involves extrapolation away from the original input space. The long-range dependence in combination with control over smoothness in the proposed covariance should be useful in dealing with such challenging applications.

## Supplementary Material

The Supplementary Material contains technical proofs and additional numerical results.

## Acknowledgements

The authors would like to thank Professor James O. Berger for commenting on an early draft of the manuscript. Bhadra gratefully acknowledges a visiting fellowship at the Statistical and Applied Mathematical Sciences Institute (SAMSI) where part of this research was conducted. This material is based upon work partially supported by the National Science Foundation under Grant DMS-1638521 to SAMSI.

## References

- Abramowitz, M. and Stegun, I. A. (1965). *Handbook of mathematical functions: with formulas, graphs, and mathematical tables*, volume 55. Courier Corporation, North Chelmsford, MA.
- Banerjee, S., Carlin, B. P., and Gelfand, A. E. (2014). *Hierarchical Modeling and Analysis for Spatial Data, Second Edition*. CRC Press, Boca Raton, FL.
- Barndorff-Nielsen, O. E. (1977). Exponentially decreasing distributions for the logarithm of particle size. *Royal Society of London Proceedings Series A* **353**, 401–419.
- Barndorff-Nielsen, O. E. (1978). Hyperbolic distributions and distributions on hyperbolae. *Scandinavian Journal of Statistics* **5**, 151–157.
- Barndorff-Nielsen, O. E., Kent, J. T., and Sørensen, M. (1982). Normal variance-mean mixtures and  $z$  distributions. *International Statistical Review* **50**, 145–159.
- Beran, J. (1992). Statistical methods for data with long-range dependence. *Statistical Science* **7**, 404–416.
- Berger, J. O. and Smith, L. A. (2019). On the statistical formalism of uncertainty quantification. *Annual Review of Statistics and Its Application* **6**, 433–460.
- Bevilacqua, M. and Faouzi, T. (2019). Estimation and prediction of Gaussian processes using generalized Cauchy covariance model under fixed domain asymptotics. *Electronic Journal of Statistics* **13**, 3025–3048.
- Bevilacqua, M., Faouzi, T., Furrer, R., and Porcu, E. (2019). Estimation and prediction using generalized Wendland covariance functions under fixed domain asymptotics. *The Annals of Statistics* **47**, 828–856.
- Bingham, N. H., Goldie, C. M., and Teugels, J. L. (1989). *Regular Variation*, volume 27 of *Encyclopedia of Mathematics and its Applications*. Cambridge University Press, Cambridge.
- Bochner, S. (1933). Monotone Funktionen, Stieltjessche Integrale und harmonische Analyse. *Mathematische Annalen* **108**, 378–410.
- Cressie, N. (1990). The origins of kriging. *Mathematical Geology* **22**, 239–252.
- Cressie, N. (1993). *Statistics for Spatial Data*. John Wiley & Sons, New York, revised edition.

- Cressie, N. (2017). Mission CO<sub>2</sub>ntrol: A statistical scientist's role in remote sensing of atmospheric carbon dioxide. *Journal of the American Statistical Association* **113**, 152–168.
- Galassi, M., Davies, J., Theiler, J., Gough, B., Jungman, G., Alken, P., Booth, M., Rossi, F., and Ulerich, R. (2002). *GNU scientific library*. Network Theory Limited.
- Gay, R. and Heyde, C. C. (1990). On a class of random field models which allows long range dependence. *Biometrika* **77**, 401–403.
- Gneiting, T. (2000). Power-law correlations, related models for long-range dependence and their simulation. *Journal of Applied Probability* **37**, 1104–1109.
- Gneiting, T. (2002). Compactly supported correlation functions. *Journal of Multivariate Analysis* **83**, 493–508.
- Gneiting, T. (2013). Strictly and non-strictly positive definite functions on spheres. *Bernoulli* **19**, 1327–1349.
- Gneiting, T. and Schlather, M. (2004). Stochastic models that separate fractal dimension and the hurst effect. *SIAM Review* **46**, 269–282.
- Gu, M., Wang, X., and Berger, J. O. (2018). Robust Gaussian stochastic process emulation. *The Annals of Statistics* **46**, 3038–3066.
- Guttorp, P. and Gneiting, T. (2006). Studies in the history of probability and statistics XLIX on the Matérn correlation family. *Biometrika* **93**, 989–995.
- Harville, D. A. (1974). Bayesian inference for variance components using only error contrasts. *Biometrika* **61**, 383–385.
- Haslett, J. and Raftery, A. E. (1989). Space-time modelling with long-memory dependence: Assessing Ireland's wind power resource. *Journal of the Royal Statistical Society: Series C (Applied Statistics)* **38**, 1–50.
- Journel, A. G. and Huijbregts, C. J. (1978). *Mining Geostatistics*. Academic Press, Cambridge, MA.
- Kaufman, C. G. and Shaby, B. A. (2013). The role of the range parameter for estimation and prediction in geostatistics. *Biometrika* **100**, 473–484.
- Matérn, B. (1960). *Spatial variation*, Meddelanden fran Statens Skogsforskningsinstitut, 49, 5. Second ed. (1986), Lecture Notes in Statistics 36, New York: Springer.
- Matheron, G. (1963). Principles of geostatistics. *Economic Geology* **58**, 1246–1266.
- Ripley, B. (1981). *Spatial Statistics*. Wiley Series in Probability and Statistics. Wiley, New York.
- Sacks, J., Welch, W. J., Mitchell, T. J., and Wynn, H. P. (1989). Design and analysis of computer experiments. *Statistical Science* **4**, 409–423.
- Santner, T. J., Williams, B. J., and Notz, W. I. (2018). *The design and analysis of computer experiments; 2nd ed.* Springer series in statistics. Springer, New York.

- Stein, M. L. (1987). Large sample properties of simulations using Latin hypercube sampling. *Technometrics* **29**, 143–151.
- Stein, M. L. (1988). Asymptotically efficient prediction of a random field with a misspecified covariance function. *The Annals of Statistics* **16**, 55–63.
- Stein, M. L. (1993). A simple condition for asymptotic optimality of linear predictions of random fields. *Statistics & Probability Letters* **17**, 399 – 404.
- Stein, M. L. (1999). *Interpolation of Spatial Data: Some Theory for Kriging*. Springer Science & Business Media, New York, NY.
- Stein, M. L. (2002). The screening effect in Kriging. *The Annals of Statistics* **30**, 298–323.
- Stein, M. L. (2005). Nonstationary spatial covariance functions. Unpublished Report. URL: [https://cfpub.epa.gov/ncer\\_abstracts/index.cfm/fuseaction/display.files/fileID/14471](https://cfpub.epa.gov/ncer_abstracts/index.cfm/fuseaction/display.files/fileID/14471).
- Stein, M. L. (2011). 2010 Rietz lecture: When does the screening effect hold? *The Annals of Statistics* **39**, 2795–2819.
- Stein, M. L. (2015). When does the screening effect not hold? *Spatial Statistics* **11**, 65–80.
- Stein, M. L. and Handcock, M. S. (1989). Some asymptotic properties of kriging when the covariance function is misspecified. *Mathematical Geology* **21**, 171–190.
- R Core Team (2018). *R: A Language and Environment for Statistical Computing*. R Foundation for Statistical Computing, Vienna, Austria.
- Wang, D. (2010). Fixed domain asymptotics and consistent estimation for Gaussian random field models in spatial statistics and computer experiments. PhD thesis, Department of Statistics and Applied Probability, National University of Singapore.
- Wang, D. and Loh, W.-L. (2011). On fixed-domain asymptotics and covariance tapering in Gaussian random field models. *Electronic Journal of Statistics* **5**, 238–269.
- Wickham, H. (2016). *ggplot2: Elegant Graphics for Data Analysis*. Springer-Verlag New York.
- Williams, C. K. and Rasmussen, C. E. (2006). *Gaussian processes for machine learning*. MIT press Cambridge, MA.
- Wunch, D., Toon, G. C., Blavier, J.-F. L., Washenfelder, R. A., Notholt, J., Connor, B. J., Griffith, D. W. T., Sherlock, V., and Wennberg, P. O. (2011). The total carbon column observing network. *Philosophical Transactions of the Royal Society A: Mathematical, Physical and Engineering Sciences* **369**, 2087–2112.
- Yadrenko, M. I. (1983). *Spectral theory of random fields*. Translation series in mathematics and engineering. Optimization Software, New York, NY. Transl. from the Russian.
- Zhang, H. (2004). Inconsistent estimation and asymptotically equal interpolations in model-based geostatistics. *Journal of the American Statistical Association* **99**, 250–261.

# Web-based Supplementary Material for Kriging: Beyond Matérn

by

Pulong Ma

Statistical and Applied Mathematical Sciences Institute and Duke University

79 T.W. Alexander Drive, P.O. Box 110207, Durham, NC 27709, USA

pulong.ma@duke.edu

and

Anindya Bhadra

Department of Statistics, Purdue University

250 N. University St., West Lafayette, IN 47907, USA

bhadra@purdue.edu

## S.1 Technical Proofs

### S.1 Proof of Theorem 1

*Proof.* As  $C(0) = \sigma^2 > 0$ , it remains to verify the positive definiteness of the function  $C(\cdot)$ . For any  $n$ , all sequences  $\{a_i \in \mathbb{R} : i = 1, \dots, n\}$  and all sequences of spatial locations  $\{\mathbf{s}_i \in \mathbb{R}^d : i = 1, \dots, n\}$ , it follows that

$$\begin{aligned} \sum_{i=1}^n \sum_{j=1}^n a_i a_j C(h_{ij}) &= \sum_{i=1}^n \sum_{j=1}^n a_i a_j \int_0^\infty \mathcal{M}(h_{ij}) \pi(\phi^2) d\phi^2 \\ &= \int_0^\infty \mathbf{a}^\top \mathbf{A} \mathbf{a} \pi(\phi^2) d\phi^2 \geq 0, \end{aligned}$$

where  $h_{ij} = \|\mathbf{s}_i - \mathbf{s}_j\|$  and  $\mathbf{a} := (a_1, \dots, a_n)^\top$ . The matrix  $\mathbf{A} := [\mathcal{M}(h_{ij})]_{i,j=1,\dots,n}$  is a covariance matrix constructed via a Matérn covariance function that is positive definite in  $\mathbb{R}^d$  for all  $d$  (Stein, 1999), and hence  $\mathbf{A}$  is a positive definite matrix, which yields that  $\mathbf{a}^\top \mathbf{A} \mathbf{a} \geq 0$ . So, the resultant integral is nonnegative, and the function  $C(h)$  is positive definite.

To derive the form of Equation (3), we start from the gamma mixture representation in Equation (2), and substitute for  $\pi(\phi^2)$  the required inverse gamma density.

$$\begin{aligned} C(h) &= \frac{\sigma^2}{2^v \Gamma(v)} \int_0^\infty x^{(v-1)} \left[ \int_0^\infty \phi^{-2v} \exp\{-x/(2\phi^2)\} \pi(\phi^2) d\phi^2 \right] \exp(-vh^2/x) dx \\ &= \frac{\sigma^2 \beta^\alpha}{2^{v+\alpha} \Gamma(v) \Gamma(\alpha)} \int_0^\infty x^{(v-1)} \left[ \int_0^\infty \phi^{-2v} \exp\{-x/(2\phi^2)\} \phi^{-2(\alpha+1)} \exp\{-\beta/(2\phi^2)\} d\phi^2 \right] \\ &\quad \times \exp(-vh^2/x) dx \\ &= \frac{\sigma^2 \beta^\alpha}{2^{v+\alpha} \Gamma(v) \Gamma(\alpha)} \int_0^\infty x^{(v-1)} \left[ \int_0^\infty \phi^{-2(v+\alpha+1)} \exp\{-(\beta+x)/(2\phi^2)\} d\phi^2 \right] \exp\{-vh^2/x\} dx \\ &= \frac{\sigma^2 \beta^\alpha \Gamma(v+\alpha)}{\Gamma(v) \Gamma(\alpha)} \int_0^\infty x^{(v-1)} (x+\beta)^{-(v+\alpha)} \exp(-vh^2/x) dx. \end{aligned}$$

□

### S.2 Proof of Theorem 2

*Proof.* (a) Using the property of modified Bessel function (see Abramowitz and Stegun, 1965, p. 375), as  $|h| \rightarrow 0$ , we can express the Matérn covariance function as

$$\mathcal{M}(h) = \begin{cases} a_1(h) + a_2(v, \sigma^2) |h|^{2v} \log |h| + O(|h|^{2v}); & \text{when } v = 0, 1, 2, \dots, \\ a_3(h) + a_4(v, \sigma^2) |h|^{2v} + O(|h|^{2\lceil v \rceil}); & \text{otherwise,} \end{cases}$$

where  $a_i(h)$ ,  $i = 1, 3$  are of the form  $\sum_{k=0}^{\lfloor v \rfloor} c_k(\phi, v, \sigma^2) h^{2k}$  with  $c_k(\phi, v, \sigma^2)$  being the coefficients that depend on parameters  $\phi, v, \sigma^2$ . The terms  $a_2(v, \sigma^2) = \frac{(-1)^{v+1} \sigma^2}{2^{2v-1} \Gamma(v) \Gamma(v+1)}$  and  $a_4(v, \sigma^2) = \frac{-\pi \sigma^2}{2^{2v} \sin(v\pi) \Gamma(v) \Gamma(v+1)}$  do not depend on  $\phi$ . The terms  $a_2(v, \sigma^2) |h|^{2v} \log |h|$  and  $a_4(v, \sigma^2) |h|^{2v}$  are called *principal irregular* terms that determine the differentiability of a random field (see Stein, 1999, p. 32). This implies that the Matérn covariance function is  $2m$  times differen-

tiable if and only if  $\nu > m$  for an integer  $m$ . By mixing the parameter  $\phi^2$  over an inverse gamma distribution, when  $h \rightarrow 0$ , the covariance function  $C(h)$  can be written as

$$C(h) = \begin{cases} \int_0^\infty a_1(h)\pi(\phi^2)d\phi^2 + a_2(\nu, \sigma^2)|h|^{2\nu} \log |h| + O(|h|^{2\nu}); & \text{when } \nu = 0, 1, 2, \dots, \\ \int_0^\infty a_3(h)\pi(\phi^2)d\phi^2 + a_4(\nu, \sigma^2)|h|^{2\nu} + O(|h|^{2\nu}); & \text{otherwise.} \end{cases}$$

Thus  $C(h)$  has the same differentiability as the Matérn covariance.

(b) It follows from Theorem 1 that

$$\begin{aligned} C(h) &= \frac{\sigma^2 \beta^\alpha \Gamma(\nu + \alpha)}{\Gamma(\nu) \Gamma(\alpha)} \int_0^\infty \left( \frac{x}{x + \beta} \right)^{\nu + \alpha} x^{-\alpha} \exp(-\nu h^2/x) dx \\ &\stackrel{t=x/2\nu}{=} \frac{\sigma^2 \Gamma(\nu + \alpha)}{(\nu/\beta)^\alpha \Gamma(\nu) \Gamma(\alpha)} \int_0^\infty t^{\nu-1} (t + \beta/(2\nu))^{-(\nu+\alpha)} \exp\{-h^2/(2t)\} dt \\ &= \frac{\sigma^2 \sqrt{2\pi} \Gamma(\nu + \alpha)}{(\nu/\beta)^\alpha \Gamma(\nu) \Gamma(\alpha)} \int_0^\infty \left( \frac{t}{t + \beta/(2\nu)} \right)^{\nu + \alpha} t^{-\alpha-1/2} \frac{1}{\sqrt{2\pi t}} \exp\{-h^2/(2t)\} dt. \end{aligned}$$

Let  $L(x) = \left( \frac{x}{x + \beta/(2\nu)} \right)^{\nu + \alpha}$ . Then  $L(x)$  is a slowly varying function. Viewed as a function of  $h$ , the above integral is a Gaussian scale mixture with respect to  $t$ . Thus, an application of Theorem 6.1 of Barndorff-Nielsen et al. (1982) yields

$$\begin{aligned} C(h) &\sim \frac{\sigma^2 \sqrt{2\pi} \Gamma(\nu + \alpha)}{(\nu/\beta)^\alpha \Gamma(\nu) \Gamma(\alpha)} (2\pi)^{-1/2} 2^{\alpha-1} \Gamma(\alpha) |h|^{-2\alpha} L(h^2), \quad \text{as } h \rightarrow \infty, \\ &= \frac{\sigma^2 2^{\alpha-1} \Gamma(\nu + \alpha)}{(\nu/\beta)^\alpha \Gamma(\nu)} |h|^{-2\alpha} L(h^2), \quad \text{as } h \rightarrow \infty. \end{aligned}$$

Thus, the tail decays as  $|h|^{-2\alpha} L(h^2)$  when  $\alpha > 0$ . □

### S.3 Proof of Theorem 3

*Proof.* Notice that the Matérn covariance function (1) has spectral density

$$\begin{aligned} f_{\mathcal{M}}(\omega) &= (2\pi)^{-d/2} \int_0^\infty (\omega h)^{-(d-2)/2} \mathcal{J}_{(d-2)/2}(\omega h) h^{d-1} \mathcal{M}(h) dh, \\ &= \frac{\sigma^2 (\sqrt{2\nu}/\phi)^{2\nu}}{\pi^{d/2} ((\sqrt{2\nu}/\phi)^2 + \omega^2)^{\nu+d/2}}, \end{aligned}$$

where  $\mathcal{J}_\nu(\cdot)$  is the ordinary Bessel function (see 9.1.20 of Abramowitz and Stegun, 1965). When  $\alpha > d/2$ , according to Bochner's Theorem (Bochner, 1933), the spectral density of the covariance function  $C(h)$  is

$$\begin{aligned} f(\omega) &= (2\pi)^{-d/2} \int_0^\infty (\omega h)^{-(d-2)/2} \mathcal{J}_{(d-2)/2}(\omega h) h^{d-1} \int_0^\infty \mathcal{M}(h) \pi(\phi^2) d\phi^2 dh \\ &= \frac{\sigma^2 2^\nu \nu^\nu (\beta/2)^\alpha}{\Gamma(\alpha)} \int_0^\infty \frac{\phi^{-2\nu}}{\pi^{d/2} (2\nu\phi^{-2} + \omega^2)^{\nu+d/2}} \phi^{-2(\alpha+1)} \exp\{-\beta/(2\phi^2)\} d\phi^2 \end{aligned}$$

$$= \frac{\sigma^2 2^{v-\alpha} \nu^v \beta^\alpha}{\pi^{d/2} \Gamma(\alpha)} \int_0^\infty (2\nu\phi^{-2} + \omega^2)^{-\nu-d/2} \phi^{-2(\nu+\alpha+1)} \exp\{-\beta/(2\phi^2)\} d\phi^2.$$

To derive the tail behavior, we make the change of variable  $\phi^2 = \beta t / \omega^2$ . The spectral density in Equation (5) can be expressed as

$$\begin{aligned} f(\omega) &= \frac{\sigma^2 2^{v-\alpha} \nu^v \beta^\alpha}{\pi^{d/2} \Gamma(\alpha)} \omega^{2\alpha-d} \int_0^\infty ((2\nu/\beta)t^{-1} + 1)^{-(\nu+d/2)} t^{-(\nu+\alpha+1)} \exp\{-\omega^2/(2t)\} dt \\ &= \frac{\sigma^2 2^{v-\alpha} \nu^v}{\pi^{d/2} \beta^v \Gamma(\alpha)} (2\pi)^{1/2} \omega^{2\alpha-d} \int_0^\infty \left( \frac{t}{2\nu/\beta + t} \right)^{(v+d/2)} t^{(-\nu-\alpha+1/2)-1} \frac{1}{\sqrt{2\pi t}} \exp\{-\omega^2/(2t)\} dt. \end{aligned}$$

Let  $L(x) = \left\{ \frac{x}{x+\beta/(2\nu)} \right\}^{v+d/2}$ . Then  $L(x)$  is a slowly varying function at  $\infty$ . The above integral is also a Gaussian scale mixture. Thus, an application of Theorem 6.1 of Barndorff-Nielsen et al. (1982) yields that as  $|\omega| \rightarrow \infty$ ,

$$\begin{aligned} f(\omega) &\sim \frac{\sigma^2 2^{v-\alpha} \nu^v}{\pi^{d/2} \beta^v \Gamma(\alpha)} (2\pi)^{1/2} \omega^{2\alpha-d} (2\pi)^{-1/2} 2^{1/2+(\nu+\alpha-1/2)} |\omega|^{-2(\nu+\alpha-1/2)-1} L(\omega^2) \\ &= \frac{\sigma^2 2^{2\nu} \nu^v \Gamma(\nu+\alpha)}{\pi^{d/2} \beta^v \Gamma(\alpha)} \omega^{-(2\nu+d)} L(\omega^2). \end{aligned}$$

□

#### S.4 Proof of Theorem 4

*Proof.* Let  $f_i(\omega), i = 1, 2$  be the spectral densities with parameters  $\{\sigma_i^2, \beta_i, \alpha_i, \nu\}$  for two covariance functions  $C_1(\cdot), C_2(\cdot)$ . The condition (6) says the spectral density  $f_i(\omega)$  is bounded at zero and  $\infty$  when  $\omega \rightarrow \infty$ . In fact, let  $\lambda = 2\nu + d$ . Then, one can show that

$$\lim_{\omega \rightarrow \infty} f_1(\omega) |\omega|^{2\nu+d} = \frac{\sigma_1^2 \beta_1^{-\nu} 2^{2\nu} \nu^v \Gamma(\nu + \alpha_1)}{\pi^{d/2} \Gamma(\alpha_1)}.$$

Thus, the condition (6) is satisfied.

We first show the sufficiency. Assume that the condition in Equation (9) holds. To prove the equivalence of two measures, it suffices to show that the condition (7) is satisfied. Notice that as  $\omega \rightarrow \infty$ ,

$$\begin{aligned} \left| \frac{f_1(\omega) - f_2(\omega)}{f_1(\omega)} \right| &= \left| \frac{\{\omega^2 + \beta_2/(2\nu)\}^{-(\nu+d/2)}}{\{\omega^2 + \beta_1/(2\nu)\}^{-(\nu+d/2)}} - 1 \right| \\ &\leq \omega^{-(2\nu+d)} \left| \{\omega^2 + \beta_2/(2\nu)\}^{\nu+d/2} - \{\omega^2 + \beta_1/(2\nu)\}^{\nu+d/2} \right| \\ &\leq \left| \{1 + (\beta_2/2\nu)\omega^{-2}\}^{\nu+d/2} - \{1 + (\beta_1/2\nu)\omega^{-2}\}^{\nu+d/2} \right| \\ &\leq \left| \{1 + (v+d/2)(\beta_2/2\nu)\omega^{-2} + O(\omega^{-4})\} \right. \\ &\quad \left. - \{1 + (v+d/2)(\beta_1/2\nu)\omega^{-2} + O(\omega^{-4})\} \right| \\ &\leq |\beta_1 - \beta_2|(v+d/2)/(2\nu)\omega^{-2} + O(\omega^{-4}). \end{aligned}$$

The integral in (7) is finite for  $d = 1, 2, 3$ . Therefore, the two measures are equivalent.

It remains to show the necessary condition. Suppose

$$\frac{\sigma_1^2 \beta_1^{-\nu} \Gamma(\nu + \alpha_1)}{\Gamma(\alpha_1)} \neq \frac{\sigma_2^2 \beta_2^{-\nu} \Gamma(\nu + \alpha_2)}{\Gamma(\alpha_2)}.$$

Let,

$$\sigma_0^2 = \sigma_2^2 \frac{\beta_2^{-\nu} \Gamma(\alpha_1) \Gamma(\nu + \alpha_2)}{\beta_1^{-\nu} \Gamma(\alpha_2) \Gamma(\nu + \alpha_1)}.$$

Then,

$$\frac{\sigma_0^2 \beta_1^{-\nu} \Gamma(\nu + \alpha_1)}{\Gamma(\alpha_1)} = \frac{\sigma_2^2 \beta_2^{-\nu} \Gamma(\nu + \alpha_2)}{\Gamma(\alpha_2)},$$

and the two covariograms  $C(h; \nu, \alpha_1, \beta_1, \sigma_0^2)$  and  $C(h; \nu, \alpha_1, \beta_1, \sigma_1^2)$  define two equivalent measures. It remains to show that  $C(h; \nu, \alpha_1, \beta_1, \sigma_0^2)$  and  $C(h; \nu, \alpha_2, \beta_2, \sigma_2^2)$  defines two equivalence Gaussian measures. The rest of arguments follow from the proof in Theorem 2 of Zhang (2004).  $\square$

## S.5 Proof of Theorem 5

*Proof.* Let  $k_1 = \sigma_1^2 \frac{2^{2\nu} \nu \Gamma(\nu + \alpha)}{\pi^{d/2} \beta^\nu \Gamma(\alpha)}$  and  $k_2 = \sigma_2^2 (2\nu)^\nu \phi^{-2\nu} / \pi^{d/2}$ . Then the condition in Equation (10) implies that  $k_1 = k_2$ . It follows that as  $|\omega| \rightarrow \infty$ ,

$$\begin{aligned} \left| \frac{f_1(\omega) - f_2(\omega)}{f_1(\omega)} \right| &= \left| \frac{k_2}{k_1} (\omega^2 + 2\nu/\phi^2)^{-(\nu+d/2)} (\omega^2 + \beta/(2\nu))^{(\nu+d/2)} - 1 \right| \\ &= (\omega^2 + 2\nu/\phi^2)^{-(\nu+d/2)} \left| k_2/k_1 (\omega^2 + 2\nu/\phi^2)^{\nu+d/2} - (\omega^2 + \beta/(2\nu))^{(\nu+d/2)} \right| \\ &\leq \omega^{-(2\nu+d)} \left| (\omega^2 + 2\nu/\phi^2)^{\nu+d/2} - (\omega^2 + \beta/(2\nu))^{\nu+d/2} \right| \\ &\leq \left| \{1 + (2\nu/\phi^2)\omega^{-2}\}^{-(\nu+d/2)} - \{1 + \beta/(2\nu)\omega^{-2}\}^{(\nu+d/2)} \right| \\ &\leq \left| \{1 + (2\nu/\phi^2)(\nu + d/2)\omega^{-2} + O(\omega^{-4})\} - \{1 + \beta/(2\nu)(\nu + d/2)\omega^{-2} + O(\omega^{-4})\} \right| \\ &\leq |2\nu/\phi^2 - \beta/(2\nu)|(\nu + d/2)\omega^{-2} + O(\omega^{-4}). \end{aligned}$$

The integral in (7) is finite for  $d = 1, 2, 3$ . Therefore, these two measures are equivalent.  $\square$

## S.6 Proof of Theorem 6

The proof of the first statement follows from the same arguments as in the proof of Theorem 3 in Zhang (2004) and is omitted. For the proof of the second statement, we follow the arguments in Wang (2010); Wang and Loh (2011) and Bevilacqua et al. (2019) to prove the asymptotic normality of the MLE for the microergodic parameter. Without loss of generality, we assume  $\mathcal{D} = [0, L]^d$ ,  $0 < L < \infty$  is a bounded subset of  $\mathbb{R}^d$  with  $d = 1, 2, 3$ . Let  $\sigma^2, \alpha, \beta$  be positive constants such that  $\sigma^2 \beta^{-\nu} \Gamma(\nu + \alpha) / \Gamma(\alpha) = \sigma_0^2 \beta_0^{-\nu} \Gamma(\nu + \alpha_0) / \Gamma(\alpha_0)$ . Let  $c(\boldsymbol{\theta}) = \sigma^2 \beta^{-\nu} \Gamma(\nu + \alpha) / \Gamma(\alpha)$  and  $\hat{c}_n(\boldsymbol{\theta}) =$

$\hat{\sigma}_n^2 \beta^{-\nu} \Gamma(\nu + \alpha) / \Gamma(\alpha)$ . Then we have

$$\sqrt{n} \{ \hat{c}_n(\boldsymbol{\theta}) - c(\boldsymbol{\theta}_0) \} = \frac{c(\boldsymbol{\theta}_0)}{\sqrt{n}} \left\{ \frac{1}{\sigma^2} \mathbf{Z}_n^\top \mathbf{R}_n^{-1}(\boldsymbol{\theta}) \mathbf{Z}_n - \frac{1}{\sigma_0^2} \mathbf{Z}_n^\top \mathbf{R}_n^{-1}(\boldsymbol{\theta}_0) \mathbf{Z}_n \right\} + \frac{c(\boldsymbol{\theta}_0)}{\sqrt{n}} \left\{ \frac{1}{\sigma_0^2} \mathbf{Z}_n^\top \mathbf{R}_n^{-1}(\boldsymbol{\theta}_0) \mathbf{Z}_n - n \right\}.$$

Under Gaussian measure  $\mathcal{P}_0$  defined by the covariance function  $C(h; \nu, \alpha_0, \beta_0, \sigma_0^2)$ , we have

$$\mathbf{Z}_n^\top \mathbf{R}_n^{-1}(\boldsymbol{\theta}_0) \mathbf{Z}_n / \sigma_0^2 \sim \chi_n^2 \quad \text{and} \quad \frac{c(\boldsymbol{\theta}_0)}{\sqrt{n}} \left\{ \frac{1}{\sigma_0^2} \mathbf{Z}_n^\top \mathbf{R}_n^{-1}(\boldsymbol{\theta}_0) \mathbf{Z}_n - n \right\} \xrightarrow{\mathcal{L}} \mathcal{N}(0, 2[c(\boldsymbol{\theta}_0)]^2),$$

as  $n \rightarrow \infty$ . To prove the result, it suffices to show that

$$\frac{1}{\sqrt{n}} \left\{ \frac{1}{\sigma^2} \mathbf{Z}_n^\top \mathbf{R}_n^{-1}(\boldsymbol{\theta}) \mathbf{Z}_n - \frac{1}{\sigma_0^2} \mathbf{Z}_n^\top \mathbf{R}_n^{-1}(\boldsymbol{\theta}_0) \mathbf{Z}_n \right\} \xrightarrow{\mathbb{P}_0} 0, \quad \text{as } n \rightarrow \infty,$$

under Gaussian measure  $\mathcal{P}_0$ . This is true if and only if for any  $\epsilon > 0$ ,

$$\begin{aligned} & \mathbb{P}_0 \left( \frac{1}{\sqrt{n}} \left| \frac{1}{\sigma^2} \mathbf{Z}_n^\top \mathbf{R}_n^{-1}(\boldsymbol{\theta}) \mathbf{Z}_n - \frac{1}{\sigma_0^2} \mathbf{Z}_n^\top \mathbf{R}_n^{-1}(\boldsymbol{\theta}_0) \mathbf{Z}_n \right| > \epsilon \right) \\ &= \mathbb{P}_0 \left( \frac{1}{\sqrt{n}} \left| \sum_{k=1}^n (\lambda_{k,n}^{-1} - 1) Y_k^2 \right| > \epsilon \right) \rightarrow 0, \quad \text{as } n \rightarrow \infty, \end{aligned}$$

where  $\mathbf{Y} := (Y_1, \dots, Y_n)^\top = \sigma_0^{-1} \mathbf{R}_n^{-1/2}(\boldsymbol{\theta}_0) \mathbf{Z}_n \sim \mathcal{N}_n(\mathbf{0}, \mathbf{I}_n)$  under  $\mathcal{P}_0$  and  $\lambda_{k,n}, k = 1, \dots, n$  are defined in the same way as in Wang (2010) and Wang and Loh (2011), satisfying

$$\sigma^2 [\sigma_0^{-1} \mathbf{R}_n^{-1/2}(\boldsymbol{\theta}_0)]^\top \mathbf{R}_n(\boldsymbol{\theta}) [\sigma_0^{-1} \mathbf{R}_n^{-1/2}(\boldsymbol{\theta}_0)] = \text{diag}\{\lambda_{k,n} : k = 1, \dots, n\}.$$

By the Markov's inequality,

$$\mathbb{P}_0 \left( \frac{1}{\sqrt{n}} \left| \sum_{k=1}^n (\lambda_{k,n}^{-1} - 1) Y_k^2 \right| > \epsilon \right) \leq \frac{1}{\epsilon \sqrt{n}} \sum_{k=1}^n |\lambda_{k,n}^{-1} - 1| \leq \frac{1}{\epsilon \sqrt{n}} \max_{1 \leq i \leq n} \sum_{k=1}^n \{\lambda_{i,n}^{-1}\} |\lambda_{k,n} - 1|.$$

The rest of the proof is to show that an upper bound of  $\frac{1}{\epsilon \sqrt{n}} \max_{1 \leq i \leq n} \sum_{k=1}^n \{\lambda_{i,n}^{-1}\} |\lambda_{k,n} - 1|$  goes to 0 as  $n \rightarrow \infty$ . The detailed arguments follow similarly to the proof of Theorem 2 of Wang and Loh (2011) and the proof of Theorem 8 of Bevilacqua et al. (2019). The key difference is that the spectral density is not that of the Matérn class or Wendland class but that of the new covariance class. As the difference between the spectral density of the Matérn class and that of the new covariance lies in a multiplicative slowly varying function, all the proofs here should follow in a similar way as in the proof of Theorem 2 of Wang and Loh (2011).

## S.7 Proof of Lemma 1

*Proof.* The difference

$$\hat{c}_n(\boldsymbol{\theta}_1) - \hat{c}_n(\boldsymbol{\theta}_2) = \mathbf{Z}_n^\top \left\{ \frac{\Gamma(\nu + \alpha_1)}{\beta_1^\nu \Gamma(\alpha_1)} \mathbf{R}_n^{-1}(\boldsymbol{\theta}_1) - \frac{\beta_2^\nu \Gamma(\nu + \alpha_2)}{\beta_2^\nu \Gamma(\alpha_2)} \mathbf{R}_n^{-1}(\boldsymbol{\theta}_2) \right\} \mathbf{Z}_n / n$$

is nonnegative for any  $\mathbf{Z}_n$  if the matrix  $\mathbf{A} := \frac{\Gamma(\nu+\alpha_1)}{\beta_1^\nu \Gamma(\alpha_1)} \mathbf{R}_n^{-1}(\boldsymbol{\theta}_1) - \frac{\Gamma(\nu+\alpha_2)}{\beta_2^\nu \Gamma(\alpha_2)} \mathbf{R}_n^{-1}(\boldsymbol{\theta}_2)$  is positive semidefinite. Notice that  $\mathbf{A}$  is positive semidefinite if and only if  $\mathbf{B} := \frac{\beta_2^\nu \Gamma(\alpha_2)}{\Gamma(\nu+\alpha_2)} \mathbf{R}_n(\boldsymbol{\theta}_2) - \frac{\beta_1^\nu \Gamma(\alpha_1)}{\Gamma(\nu+\alpha_1)} \mathbf{R}_n(\boldsymbol{\theta}_1)$  is positive semidefinite. The entries of  $\mathbf{B}$  can be expressed in terms of a function  $K_B : \mathbb{R}^d \rightarrow \mathbb{R}$ , with

$$B_{ij} = K_B(\mathbf{s}_i - \mathbf{s}_j) = \frac{\beta_2^\nu \Gamma(\alpha_2)}{\Gamma(\nu + \alpha_2)} R(\|\mathbf{s}_i - \mathbf{s}_j\|; \alpha_2, \beta_2, \nu) - \frac{\beta_1^\nu \Gamma(\alpha_1)}{\Gamma(\nu + \alpha_1)} R(\|\mathbf{s}_i - \mathbf{s}_j\|; \alpha_1, \beta_1, \nu),$$

and the matrix  $\mathbf{B}$  is positive semidefinite if  $K_B$  is a positive definite function. Define its Fourier transform by

$$\begin{aligned} f_B(\boldsymbol{\omega}) &= \frac{1}{(2\pi)^d} \int_{\mathbb{R}^d} \exp\{-i\boldsymbol{\omega}^\top x\} K_B(x) dx \\ &= \frac{\beta_2^\nu \Gamma(\alpha_2)}{\Gamma(\nu + \alpha_2)} \left\{ \frac{1}{(2\pi)^d} \int_{\mathbb{R}^d} \exp\{-i\boldsymbol{\omega}^\top x\} R(x; \alpha_2, \beta_2, \nu) dx \right\} \\ &\quad - \frac{\beta_1^\nu \Gamma(\alpha_1)}{\Gamma(\nu + \alpha_1)} \left\{ \frac{1}{(2\pi)^d} \int_{\mathbb{R}^d} \exp\{-i\boldsymbol{\omega}^\top x\} R(x; \alpha_1, \beta_1, \nu) dx \right\}. \end{aligned}$$

The integrals in  $f_B(\boldsymbol{\omega})$  are finite with  $g(\boldsymbol{\omega}) := \frac{1}{(2\pi)^d} \int_{\mathbb{R}^d} \exp\{-i\boldsymbol{\omega}^\top x\} R(x; \alpha, \beta, \nu) dx$  being the spectral density of the new correlation function with parameters  $\alpha, \beta, \nu$ , given by

$$g(\boldsymbol{\omega}) = \frac{2^{2\nu} \nu^\nu}{\pi^{d/2} \beta^\nu \Gamma(\alpha)} \int_0^\infty \{4\nu/(\beta t) + \|\boldsymbol{\omega}\|^2\}^{-(\nu+d/2)} t^{-(\nu+\alpha+1)} \exp\{-1/t\} dt.$$

Thus,  $K_B$  is positive definite if  $f_B$  is positive for all  $\boldsymbol{\omega}$ . Notice that  $f_B$  is given by

$$\begin{aligned} f_B(\boldsymbol{\omega}) &= \frac{(4\nu)^\nu}{\pi^{d/2} \Gamma(\nu + \alpha_2)} \int_0^\infty \{4\nu/(\beta_2 t) + \|\boldsymbol{\omega}\|^2\}^{-(\nu+d/2)} t^{-(\nu+\alpha_2+1)} \exp\{-1/t\} dt \\ &\quad - \frac{(4\nu)^\nu}{\pi^{d/2} \Gamma(\nu + \alpha_1)} \int_0^\infty \{4\nu/(\beta_1 t) + \|\boldsymbol{\omega}\|^2\}^{-(\nu+d/2)} t^{-(\nu+\alpha_1+1)} \exp\{-1/t\} dt. \end{aligned}$$

It is straightforward to check that when  $\alpha := \alpha_1 = \alpha_2 > d/2$ ,

$$\beta_1 < \beta_2 \implies f_B(\boldsymbol{\omega}) > 0 \quad \text{for all } \boldsymbol{\omega}.$$

Thus, if  $\beta_1 < \beta_2$ , then  $\hat{c}_n(\alpha, \beta_1) \leq \hat{c}_n(\alpha, \beta_2)$ .

The proof of the second statement is as follows. Note that the integral inside  $f_B(\boldsymbol{\omega})$  can be expressed as

$$\begin{aligned} I(\alpha) &:= \int_0^\infty \{4\nu/(\beta t) + \|\boldsymbol{\omega}\|^2\}^{-(\nu+d/2)} t^{-(\nu+\alpha+1)} \exp\{-1/t\} dt \\ &= \int_0^\infty \frac{u^{\nu+\alpha-1}}{\Gamma(\nu + \alpha)} \exp\{-u\} (4\nu u/\beta + \|\boldsymbol{\omega}\|^2) du \\ &= E_U (4\nu u/\beta + \|\boldsymbol{\omega}\|^2)^{-(\nu+d/2)}, \end{aligned}$$

where  $U \sim \text{Gamma}(\nu + \alpha, 1)$ . This expectation is finite if  $\alpha > d/2$ . Suppose that  $\alpha_1 < \alpha_2$  and  $\beta := \beta_1 = \beta_2$ . To show  $f_B(\boldsymbol{\omega})$  is negative for all  $\boldsymbol{\omega}$ , it suffices to show that  $I(\alpha_2) - I(\alpha_1) \leq 0$ . Let  $U_1 \sim \text{Gamma}(\nu + \alpha_1, 1)$  and  $U_2 \sim \text{Gamma}(\nu + \alpha_2, 1)$ . Then  $U_2 = U_1 + U_0$ , where  $U_0 \sim$

$\text{Gamma}(\alpha_2 - \alpha_1, 1)$  and  $U_0$  is independent of  $U_1$ . Thus, the quantify  $I(\alpha_2)$  can be upper bounded by  $I(\alpha_1)$ , since,

$$\begin{aligned} I(\alpha_2) &= E_{U_1, U_0} \left\{ \frac{4v}{\beta} (U_1 + U_0) + \|\boldsymbol{\omega}\|^2 \right\}^{-(v+d/2)} = E_{U_1, U_0} \left\{ \frac{4v}{\beta} U_1 + \|\boldsymbol{\omega}\|^2 + \frac{4v}{\beta} U_0 \right\}^{-(v+d/2)} \\ &\leq E_{U_1} \left\{ \frac{4v}{\beta} U_1 + \|\boldsymbol{\omega}\|^2 \right\}^{-(v+d/2)} = I(\alpha_1). \end{aligned}$$

□

## S.8 Proof of Corollary 2

*Proof.* The proof is analogous to the proof of Theorem 4 in Kaufman and Shaby (2013). Let

$$\sigma_1^2 := \sigma_0^2 (\beta_1 / \beta_0)^v \frac{\Gamma(v + \alpha_0) \Gamma(\alpha_1)}{\Gamma(v + \alpha_1) \Gamma(\alpha_0)}.$$

Then  $\mathcal{P}_0$  and  $\mathcal{P}_1$  define two equivalence measures. We write

$$\frac{\text{Var}_{v, \boldsymbol{\theta}_1, \hat{\sigma}_n^2} \{ \hat{Z}_n(\boldsymbol{\theta}_1) - Z(\mathbf{s}_0) \}}{\text{Var}_{v, \boldsymbol{\theta}_0, \sigma_0^2} \{ \hat{Z}_n(\boldsymbol{\theta}_1) - Z(\mathbf{s}_0) \}} = \frac{\text{Var}_{v, \boldsymbol{\theta}_1, \hat{\sigma}_n^2} \{ \hat{Z}_n(\boldsymbol{\theta}_1) - Z(\mathbf{s}_0) \}}{\text{Var}_{v, \boldsymbol{\theta}_1, \sigma_1^2} \{ \hat{Z}_n(\boldsymbol{\theta}_1) - Z(\mathbf{s}_0) \}} \frac{\text{Var}_{v, \boldsymbol{\theta}_1, \sigma_1^2} \{ \hat{Z}_n(\boldsymbol{\theta}_1) - Z(\mathbf{s}_0) \}}{\text{Var}_{v, \boldsymbol{\theta}_0, \sigma_0^2} \{ \hat{Z}_n(\boldsymbol{\theta}_1) - Z(\mathbf{s}_0) \}}.$$

According to Part (b) of Theorem 8, it suffices to show that almost surely

$$\frac{\text{Var}_{v, \boldsymbol{\theta}_1, \hat{\sigma}_n^2} \{ \hat{Z}_n(\boldsymbol{\theta}_1) - Z(\mathbf{s}_0) \}}{\text{Var}_{v, \boldsymbol{\theta}_1, \sigma_1^2} \{ \hat{Z}_n(\boldsymbol{\theta}_1) - Z(\mathbf{s}_0) \}} \rightarrow 1.$$

By Equation (13),

$$\frac{\text{Var}_{v, \boldsymbol{\theta}_1, \hat{\sigma}_n^2} \{ \hat{Z}_n(\boldsymbol{\theta}_1) - Z(\mathbf{s}_0) \}}{\text{Var}_{v, \boldsymbol{\theta}_1, \sigma_1^2} \{ \hat{Z}_n(\boldsymbol{\theta}_1) - Z(\mathbf{s}_0) \}} = \frac{\hat{\sigma}_n^2}{\sigma_1^2}.$$

Note that under  $\mathcal{P}_1$ , we have  $\hat{\sigma}_n^2 \sim (\sigma_0^2/n)\chi_n$ , and hence  $\hat{\sigma}_n^2$  converges almost surely to  $\sigma_0^2$  as  $n \rightarrow \infty$ . As  $\mathcal{P}_0$  is equivalent to  $\mathcal{P}_1$ , It follows from Theorem 6 that  $\hat{\sigma}_n^2 \rightarrow \sigma_1^2$ , almost surely. □

## S.2 Additional Simulation Examples

### S.1 Predictive Performance with Different Sample Sizes

In this section, we use the same simulation settings as in Section 4 but with  $n = 500$  and 1000 observations for parameter estimation. The simulation setup here is the same as the one considered in Section 4.1. For  $n = 500$  observations, the results are shown in Figure S.1 for Case 1, Figure S.2 for Case 2, and Figure S.3 for Case 3. For  $n = 1000$  observations, the results are shown in Figure S.4 for Case 1, Figure S.5 for Case 2, and Figure S.6 for Case 3. To conclude, the new covariance class is very flexible since it can allow different smoothness behaviors in the same way as the Matérn class and can allow different degrees of tail behaviors that can capture the one in the GC class.

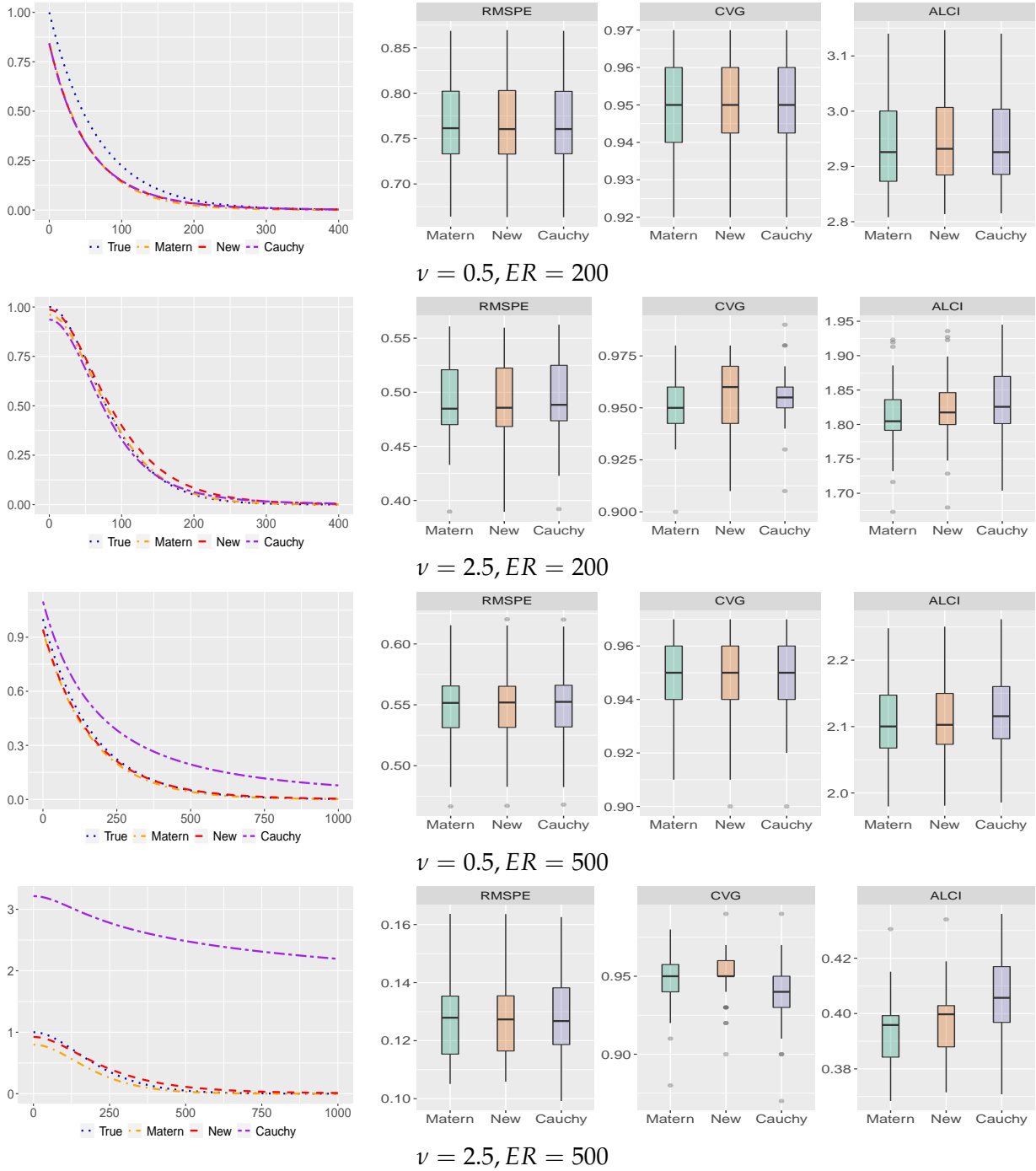


**Fig. S.1.** Case 1: Comparison of predictive performance and estimated covariance structures when the true covariance is the Matérn class with 500 observations. The predictive performance is evaluated at 10-by-10 regular grids in the square domain. These figures summarize the predictive measures based on RMSPE, CVG and ALCI under 30 simulated realizations.

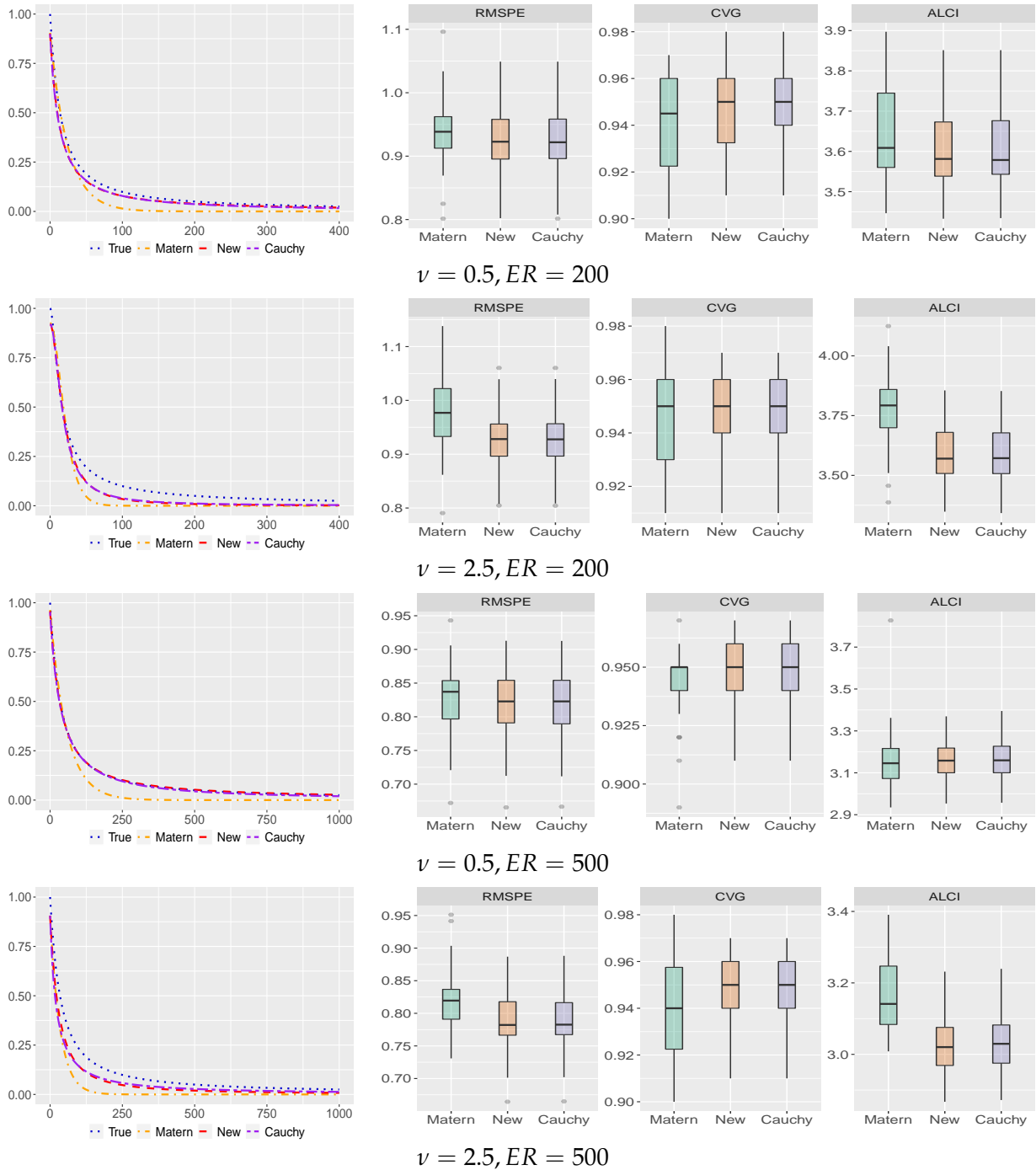


**Fig. S.2.** Case 2: Comparison of predictive performance and estimated covariance structures when the true covariance is the new covariance class with 500 observations. The predictive performance is evaluated at 10-by-10 regular grids in the square domain. These figures summarize the predictive measures based on RMSPE, CVG and ALCI under 30 simulated realizations.

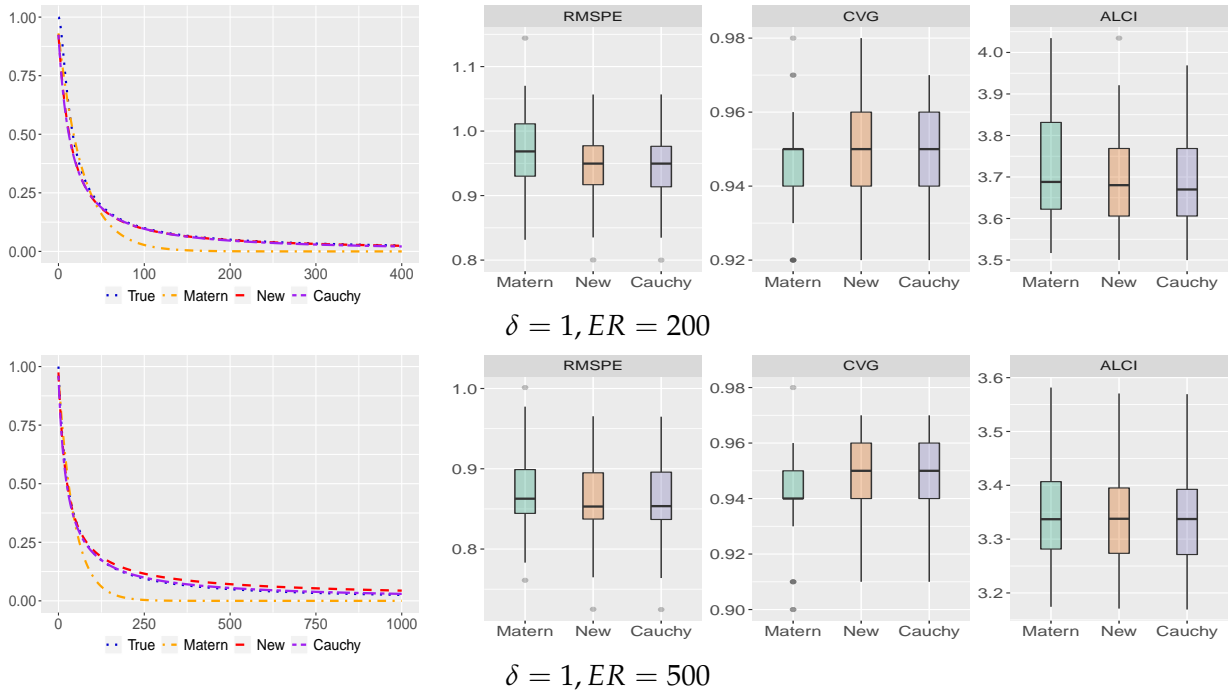


**Fig. S.3.** Case 3: Comparison of predictive performance and estimated covariance structures when the true covariance is the GC class with 500 observations. The predictive performance is evaluated at 10-by-10 regular grids in the square domain. These figures summarize the predictive measures based on RMSPE, CVG and ALCI under 30 simulated realizations.

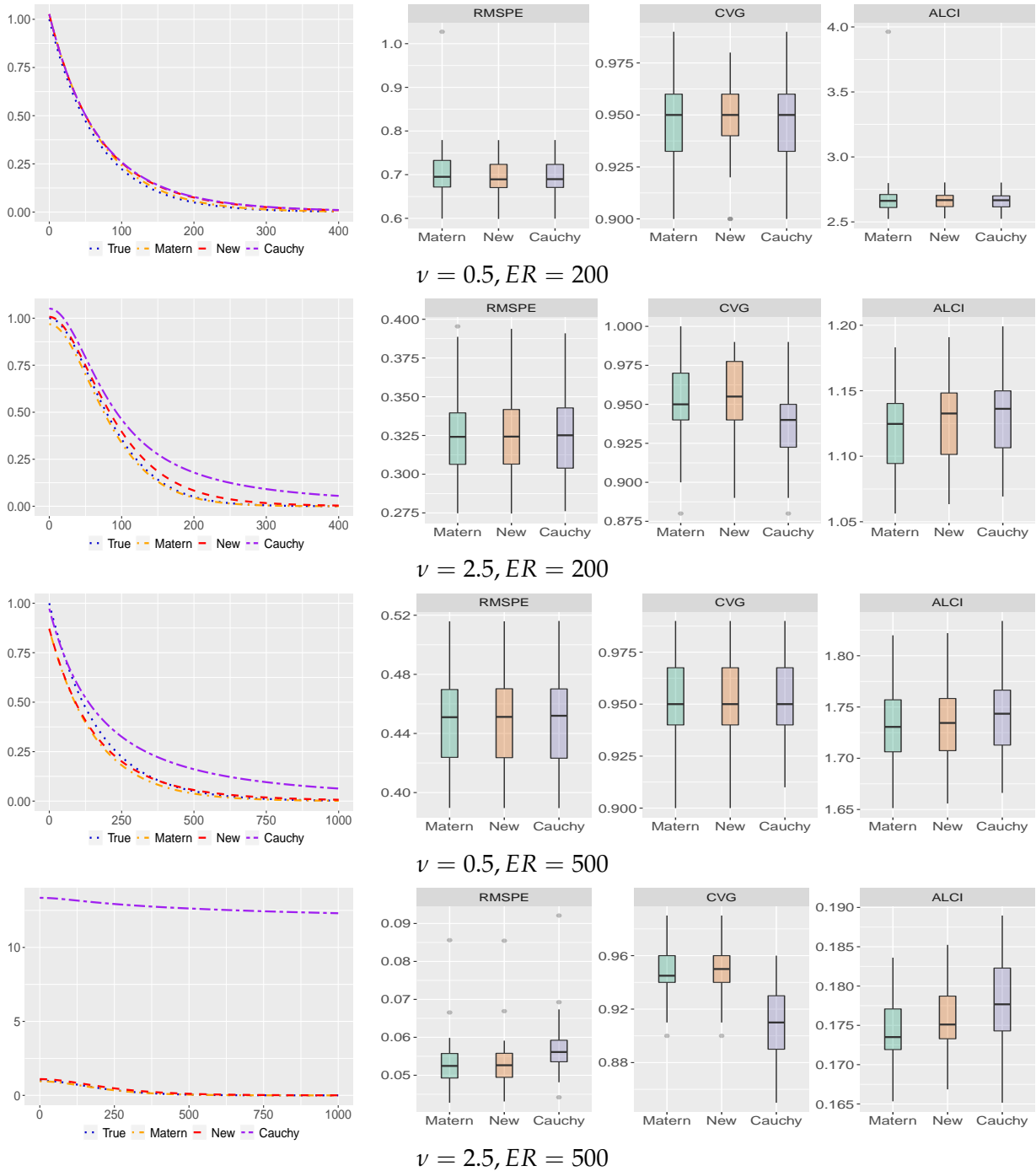


**Fig. S.4.** Case 1: Comparison of predictive performance and estimated covariance structures when the true covariance is the Matérn class with 1000 observations. The predictive performance is evaluated at 10-by-10 regular grids in the square domain. These figures summarize the predictive measures based on RMSPE, CVG and ALCI under 30 simulated realizations.

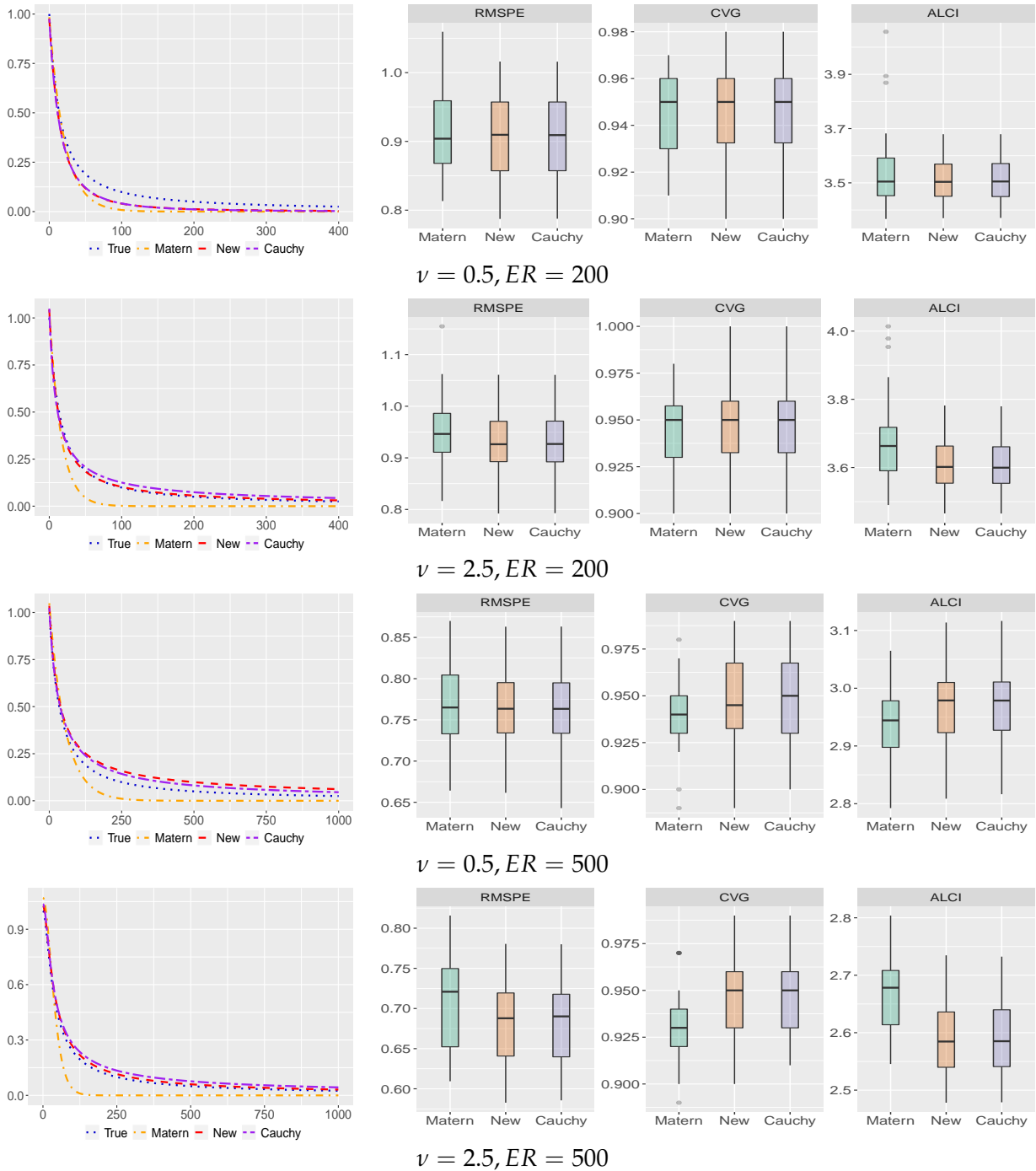


**Fig. S.5.** Case 2: Comparison of predictive performance and estimated covariance structures when the true covariance is the new covariance class with 1000 observations. The predictive performance is evaluated at 10-by-10 regular grids in the square domain. These figures summarize the predictive measures based on RMSPE, CVG and ALCI under 30 simulated realizations.

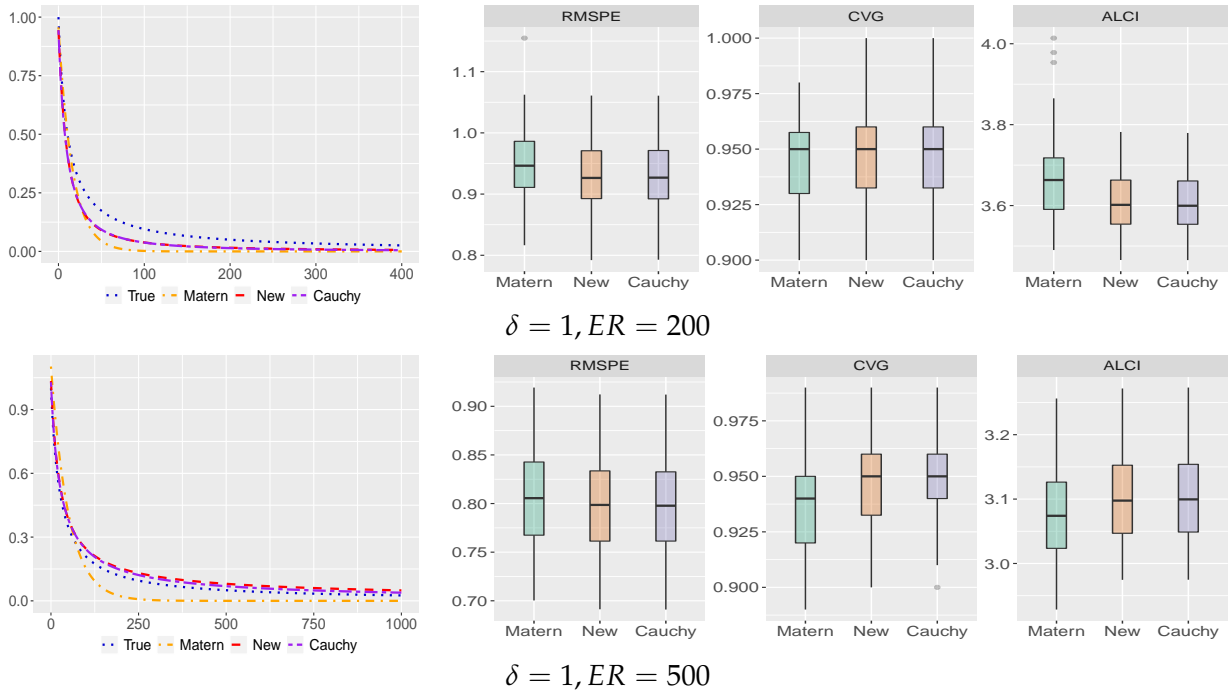


**Fig. S.6.** Case 3: Comparison of predictive performance and estimated covariance structures when the true covariance is the GC class with 1000 observations. The predictive performance is evaluated at 10-by-10 regular grids in the square domain. These figures summarize the predictive measures based on RMSPE, CVG and ALCI under 30 simulated realizations.

## S.2 Simulation with a Product Form of Covariance Functions

In this section, we study the predictive performance of the new covariance function with a product form, i.e.,  $r(\|\mathbf{s} - \mathbf{u}\|) = \prod_{i=1}^d R(|s_i - u_i|; \theta_i)$ , where  $R(\cdot; \theta_i)$  is an isotropic covariance function with parameter  $\theta_i$ . This product form of covariance functions allows different properties along different coordinate directions (or input space) and has been widely used in uncertainty quantification and machine learning.

We simulate the true processes under the Matérn class and the new covariance class with effective range fixed at 200 and 500. For the smoothness parameter, we consider  $\nu = 0.5, 2.5$ . The tail decay parameter in the new covariance class is chosen to be 0.5. As each dimension has a different range parameter or scale parameter, we choose these parameters in each dimension such that their correlation will be  $0.5^{1/2}$  at distance 200 and 500. This will guarantee the overall effective range will be 200 and 500, respectively. For each simulation setting, the true process is simulated at  $n = 100, 500, 1000$  locations. The GC class has a smoothness parameter that is specified as in Section 4.1. The prediction locations are the same as those in Section 4.1.

In the first case where the true process has a product of Matérn covariance functions, the prediction results under the Matérn class, the new covariance class and the GC class are shown in panels from (a) to (f) of Figure S.7. As we can expected, the Matérn class and the new covariance class yield indistinguishable predictive performance in terms of RMSPE, CVG, and ALCI. However, the GC class has much worse performance than the other two covariance classes. In the second case where the true process has a product of new covariance functions, the prediction results under these three covariance classes are shown in panels from (g) to (l) of Figure S.7. As expected, the new covariance class yields slightly better prediction results than the Matérn class, since the Matérn class has an exponentially decaying tail that is not able to capture the tail behavior in the new covariance class. It is worth noting that the GC class yields much worse predictive performance than the other two covariance classes. This is quite different from the situation when the true process does not have a product covariance form.

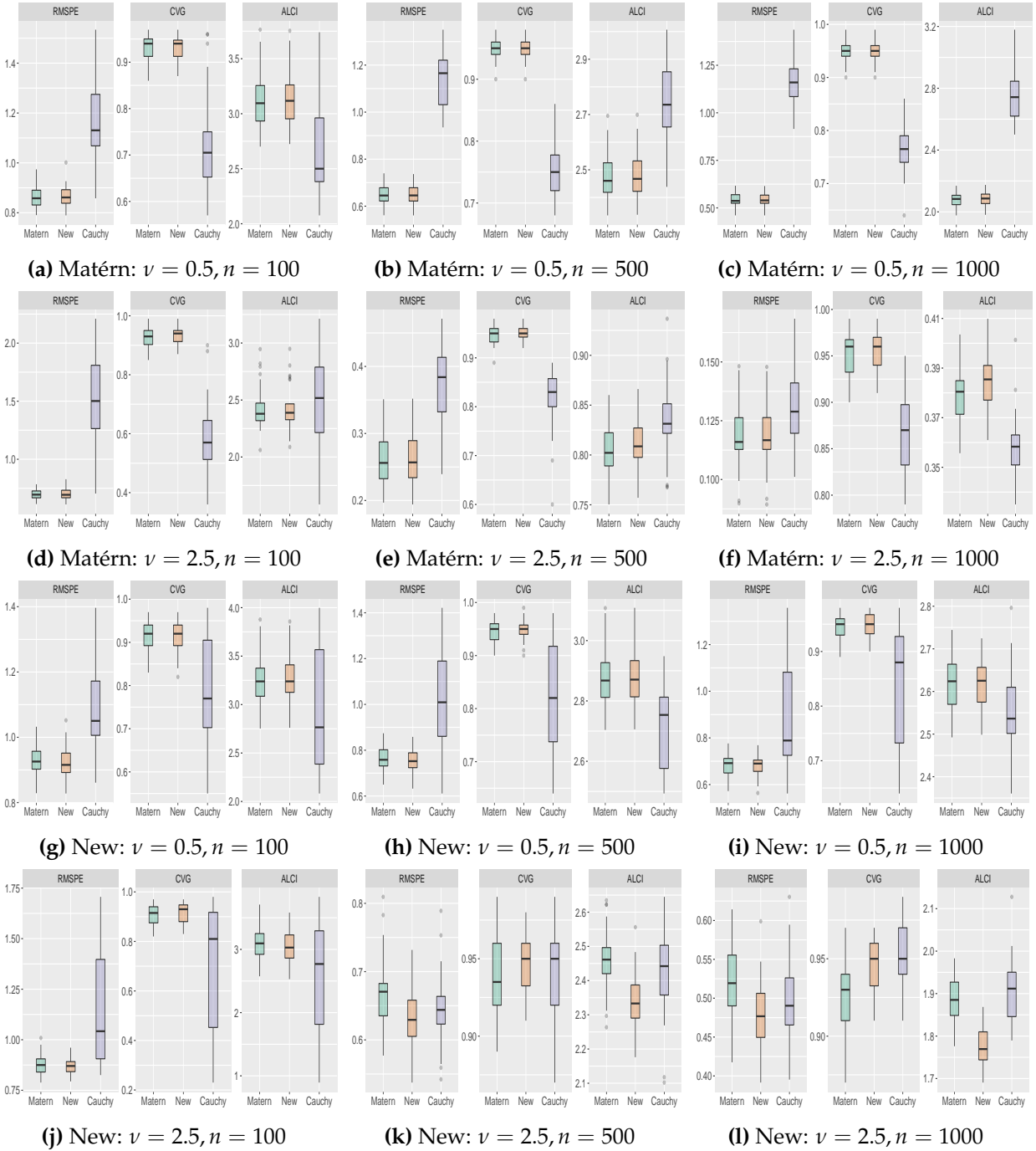


**Fig. S.7.** Predictive performance over 10-by-10 regular grids under three covariance classes when the true process has a product form of covariance structures. The predictive performance is studied under different smoothness parameters, effective Cauchy ranges and number of observation locations.

### S.3 Additional Numerical Results

This section contains additional simulation results referenced in Section 4.2 and parameter estimation results referenced in Section 5. Table S.1, Table S.2 and Table S.3 show the percentiles of  $\xi$ , CVG, bias, and RMSE of  $\hat{c}_n(\boldsymbol{\theta})$ , where  $\boldsymbol{\theta} = (\alpha_0, \beta_0)$ ,  $\boldsymbol{\theta} = (\alpha_0, 0.5\beta_0)$ ,  $\boldsymbol{\theta} = (\alpha_0, 2\beta_0)$ ,  $\boldsymbol{\theta} = (\alpha_0, \hat{\beta}_n)$ , and  $\boldsymbol{\theta} = (\hat{\alpha}_n, \hat{\beta}_n)$  for  $\nu \in \{0.5, 1.5\}$ ,  $\alpha \in \{0.5, 2, 5\}$ ,  $ER \in \{0.6, 0.9\}$  with  $n = 4000, 5000, 6000$ . Table S.4 shows the estimated parameters under the Matérn covariance model and the new covariance model in the cross-validation study of Section 5.

**Table S.1.** Percentiles of  $\zeta$  and CVG, bias, and RMSE of  $\hat{c}_n(\theta)$  when  $\alpha_0 = 0.5$ .

Settings		5%	25%	50%	75%	95%	CVG	bias	RMSE
$\mathcal{N}(0,1)$		-1.6449	-0.6749	0	0.6749	1.6449	0.95	0	
$ER = 0.6, \nu = 0.5$									
$\theta$									
$\alpha = \alpha_0, \beta = \beta_0$	$n = 4000$	-1.449	-0.542	0.009	0.686	1.767	0.955	0.020	0.327
	$n = 5000$	-1.469	-0.665	-0.077	0.696	1.573	0.965	-0.003	0.289
	$n = 6000$	-1.705	-0.618	0.056	0.662	1.847	0.929	0.010	0.280
$\alpha = \alpha_0, \beta = 0.5\beta_0$	$n = 4000$	2.113	3.098	3.730	4.424	5.549	0.044	1.259	1.308
	$n = 5000$	2.129	2.930	3.578	4.439	5.347	0.040	1.097	1.140
	$n = 6000$	1.798	3.015	3.705	4.397	5.606	0.071	1.005	1.049
$\alpha = \alpha_0, \beta = 2\beta_0$	$n = 4000$	-3.471	-2.608	-2.073	-1.420	-0.394	0.415	-0.676	0.746
	$n = 5000$	-3.480	-2.693	-2.114	-1.395	-0.519	0.404	-0.611	0.676
	$n = 6000$	-3.688	-2.623	-1.967	-1.376	-0.214	0.462	-0.543	0.606
$\alpha = \alpha_0, \beta = \hat{\beta}_n$	$n = 4000$	-1.871	-0.711	0.095	1.000	2.244	0.889	0.047	0.428
	$n = 5000$	-1.912	-0.767	0.022	0.881	2.134	0.881	0.013	0.371
	$n = 6000$	-2.016	-0.760	0.096	0.862	2.097	0.879	0.019	0.343
$\alpha = \hat{\alpha}_n, \beta = \hat{\beta}_n$	$n = 4000$	-1.778	-0.875	0.000	0.925	2.382	0.887	0.030	0.446
	$n = 5000$	-2.129	-0.816	0.026	0.893	2.227	0.870	0.019	0.395
	$n = 6000$	-2.268	-0.911	-0.015	0.865	2.117	0.875	-0.006	0.363
$ER = 0.6, \nu = 1.5$									
$\theta$									
$\alpha = \alpha_0, \beta = \beta_0$	$n = 4000$	-1.654	-0.604	-0.014	0.701	1.776	0.949	12.650	370.7
	$n = 5000$	-1.430	-0.687	-0.046	0.672	1.576	0.969	0.283	312.0
	$n = 6000$	-1.731	-0.649	0.070	0.710	1.740	0.929	7.182	307.5
$\alpha = \alpha_0, \beta = 0.5\beta_0$	$n = 4000$	26.20	27.77	28.82	30.03	31.76	0.000	10495	10513
	$n = 5000$	27.09	28.35	29.37	30.55	31.99	0.000	9567	9581
	$n = 6000$	27.22	28.79	29.85	30.89	32.68	0.000	8860	8874
$\alpha = \alpha_0, \beta = 2\beta_0$	$n = 4000$	-13.70	-12.93	-12.48	-11.99	-11.21	0.000	-4526	4534
	$n = 5000$	-13.99	-13.35	-12.90	-12.36	-11.62	0.000	-4177	4184
	$n = 6000$	-14.47	-13.61	-13.11	-12.58	-11.80	0.000	-3886	3893
$\alpha = \alpha_0, \beta = \hat{\beta}_n$	$n = 4000$	-2.993	-1.121	0.172	1.515	3.505	0.670	72.52	732.5
	$n = 5000$	-2.823	-1.155	0.146	1.452	3.398	0.700	49.49	624.8
	$n = 6000$	-3.068	-1.090	0.235	1.433	3.093	0.733	44.59	543.1
$\alpha = \hat{\alpha}_n, \beta = \hat{\beta}_n$	$n = 4000$	-3.887	-1.656	0.061	1.681	4.142	0.565	9.059	895.5
	$n = 5000$	-3.607	-1.643	0.055	1.497	4.142	0.592	16.27	772.1
	$n = 6000$	-4.107	-1.678	-0.206	1.488	3.774	0.592	-70.59	832.3
$ER = 0.9, \nu = 0.5$									
$\theta$									
$\alpha = \alpha_0, \beta = \beta_0$	$n = 4000$	-1.589	-0.557	-0.013	0.669	1.748	0.955	0.007	0.220
	$n = 5000$	-1.429	-0.654	0.065	0.759	1.683	0.978	0.012	0.190
	$n = 6000$	-1.512	-0.591	0.004	0.702	1.768	0.943	0.009	0.179
$\alpha = \alpha_0, \beta = 0.5\beta_0$	$n = 4000$	0.628	1.679	2.278	2.967	4.052	0.399	0.513	0.563
	$n = 5000$	0.727	1.546	2.306	2.994	3.958	0.420	0.454	0.496
	$n = 6000$	0.548	1.543	2.200	2.888	4.013	0.445	0.403	0.444
$\alpha = \alpha_0, \beta = 2\beta_0$	$n = 4000$	-2.812	-1.808	-1.259	-0.595	0.440	0.769	-0.272	0.346
	$n = 5000$	-2.620	-1.846	-1.170	-0.478	0.379	0.760	-0.229	0.295
	$n = 6000$	-2.635	-1.756	-1.187	-0.477	0.586	0.799	-0.205	0.270
$\alpha = \alpha_0, \beta = \hat{\beta}_n$	$n = 4000$	-1.856	-0.688	0.087	0.911	1.946	0.905	0.021	0.262
	$n = 5000$	-1.587	-0.696	0.062	0.822	1.930	0.926	0.018	0.220
	$n = 6000$	-1.646	-0.589	0.045	0.833	2.008	0.918	0.020	0.202
$\alpha = \hat{\alpha}_n, \beta = \hat{\beta}_n$	$n = 4000$	-1.876	-0.748	0.082	0.882	2.157	0.887	0.016	0.276
	$n = 5000$	-1.865	-0.692	0.023	0.853	1.994	0.902	0.014	0.233
	$n = 6000$	-1.884	-0.744	0.006	0.901	1.978	0.904	0.008	0.213
$ER = 0.9, \nu = 1.5$									
$\theta$									
$\alpha = \alpha_0, \beta = \beta_0$	$n = 4000$	-1.598	-0.618	-0.015	0.663	1.747	0.958	2.284	106.8
	$n = 5000$	-1.426	-0.647	0.063	0.774	1.711	0.977	6.598	92.45
	$n = 6000$	-1.660	-0.623	0.059	0.685	1.743	0.945	2.287	87.41
$\alpha = \alpha_0, \beta = 0.5\beta_0$	$n = 4000$	17.15	18.51	19.42	20.44	21.94	0.000	2096	2102
	$n = 5000$	17.34	18.50	19.50	20.42	21.83	0.000	1877	1881
	$n = 6000$	17.06	18.45	19.36	20.24	21.70	0.000	1699	1703
$\alpha = \alpha_0, \beta = 2\beta_0$	$n = 4000$	-10.02	-9.207	-8.722	-8.151	-7.284	0.000	-934.2	938.3
	$n = 5000$	-9.964	-9.263	-8.691	-8.092	-7.331	0.000	-8.835	839.5
	$n = 6000$	-10.13	-9.280	-8.717	-8.159	-7.26	0.000	-766.2	769.8
$\alpha = \alpha_0, \beta = \hat{\beta}_n$	$n = 4000$	-2.455	-0.993	0.029	1.282	2.953	0.771	15.62	180.4
	$n = 5000$	-2.224	-1.038	-0.031	1.140	2.706	0.789	8.661	151.8
	$n = 6000$	-2.259	-0.918	0.082	1.152	2.586	0.803	11.20	131.2
$\alpha = \hat{\alpha}_n, \beta = \hat{\beta}_n$	$n = 4000$	-3.178	-1.316	-0.002	1.215	3.289	0.691	1.887	208.8
	$n = 5000$	-3.055	-1.211	-0.003	1.229	3.129	0.708	2.440	178.3
	$n = 6000$	-2.820	-1.285	0.006	1.236	3.051	0.710	0.875	156.7

**Table S.2.** Percentiles of  $\zeta$  and CVG, bias, and RMSE of  $\hat{c}_n(\theta)$  when  $\alpha_0 = 2$ .

Settings		5%	25%	50%	75%	95%	CVG	bias	RMSE
$\mathcal{N}(0,1)$		-1.6449	-0.6749	0	0.6749	1.6449	0.95	0	
$ER = 0.6, v = 0.5$									
$\theta$									
$\alpha = \alpha_0, \beta = \beta_0$	$n = 4000$	-1.557	-0.604	-0.013	0.691	1.759	0.954	0.004	0.099
	$n = 5000$	-1.442	-0.614	0.003	0.723	1.575	0.962	0.002	0.086
	$n = 6000$	-1.689	-0.462	0.093	0.728	1.970	0.947	0.003	0.084
$\alpha = \alpha_0, \beta = 0.5\beta_0$	$n = 4000$	-1.072	-0.128	0.486	1.179	2.264	0.921	0.052	0.113
	$n = 5000$	-0.999	-0.179	0.493	1.183	2.047	0.939	0.043	0.097
	$n = 6000$	-1.315	-0.010	0.556	1.184	2.396	0.929	0.041	0.094
$\alpha = \alpha_0, \beta = 2\beta_0$	$n = 4000$	-1.801	-0.860	-0.258	0.440	1.505	0.949	-0.021	0.101
	$n = 5000$	-1.680	-0.840	-0.232	0.479	1.347	0.946	-0.018	0.088
	$n = 6000$	-1.880	-0.681	-0.136	0.517	1.756	0.931	-0.012	0.084
$\alpha = \alpha_0, \beta = \hat{\beta}_n$	$n = 4000$	-1.616	-0.600	0.040	0.758	1.796	0.954	0.008	0.103
	$n = 5000$	-1.443	-0.583	0.070	0.752	1.705	0.962	0.006	0.088
	$n = 6000$	-1.564	-0.505	0.171	0.774	1.941	0.938	0.008	0.087
$\alpha = \hat{\alpha}_n, \beta = \hat{\beta}_n$	$n = 4000$	-1.576	-0.546	0.140	0.798	1.880	0.944	0.014	0.104
	$n = 5000$	-1.426	-0.565	0.094	0.785	1.747	0.956	0.009	0.089
	$n = 6000$	-1.595	-0.614	0.079	0.764	1.882	0.953	0.007	0.085
$ER = 0.6, v = 1.5$									
$\theta$									
$\alpha = \alpha_0, \beta = \beta_0$	$n = 4000$	-1.567	-0.624	-0.010	0.689	1.764	0.952	0.103	2.513
	$n = 5000$	-1.469	-0.633	0.005	0.734	1.620	0.958	0.083	2.200
	$n = 6000$	-1.729	-0.614	0.016	0.592	1.646	0.953	-0.013	2.027
$\alpha = \alpha_0, \beta = 0.5\beta_0$	$n = 4000$	1.226	2.227	2.885	3.622	4.748	0.215	7.351	7.840
	$n = 5000$	1.056	2.005	2.772	3.469	4.427	0.257	6.145	6.586
	$n = 6000$	0.725	1.861	2.602	3.180	4.350	0.296	5.225	5.657
$\alpha = \alpha_0, \beta = 2\beta_0$	$n = 4000$	-2.801	-1.876	-1.283	-0.593	0.433	0.749	-3.103	3.948
	$n = 5000$	-2.590	-1.829	-1.185	-0.497	0.385	0.765	-2.612	3.379
	$n = 6000$	-2.807	-1.771	-1.128	-0.565	0.493	0.779	-2.350	3.073
$\alpha = \alpha_0, \beta = \hat{\beta}_n$	$n = 4000$	-1.613	-0.649	0.093	0.790	1.923	0.928	0.223	2.701
	$n = 5000$	-1.417	-0.648	0.046	0.818	1.821	0.957	0.197	2.332
	$n = 6000$	-1.623	-0.655	0.056	0.691	1.793	0.954	0.071	2.111
$\alpha = \hat{\alpha}_n, \beta = \hat{\beta}_n$	$n = 4000$	-1.558	-0.598	0.095	0.811	1.977	0.921	0.301	2.759
	$n = 5000$	-1.543	-0.594	0.040	0.798	1.827	0.950	0.186	2.342
	$n = 6000$	-1.604	-0.569	0.090	0.763	1.827	0.946	0.198	2.132
$ER = 0.9, v = 0.5$									
$\theta$									
$\alpha = \alpha_0, \beta = \beta_0$	$n = 4000$	-1.574	-0.594	-0.026	0.666	1.776	0.952	0.002	0.066
	$n = 5000$	-1.458	-0.664	-0.052	0.638	1.547	0.962	-0.001	0.057
	$n = 6000$	-1.742	-0.548	0.145	0.809	1.784	0.942	0.005	0.055
$\alpha = \alpha_0, \beta = 0.5\beta_0$	$n = 4000$	-1.319	-0.321	0.254	0.930	2.042	0.938	0.020	0.069
	$n = 5000$	-1.220	-0.411	0.185	0.904	1.817	0.962	0.014	0.059
	$n = 6000$	-1.567	-0.366	0.385	1.022	2.052	0.925	0.017	0.058
$\alpha = \alpha_0, \beta = 2\beta_0$	$n = 4000$	-1.704	-0.723	-0.158	0.524	1.635	0.950	-0.007	0.066
	$n = 5000$	-1.579	-0.786	-0.173	0.517	1.424	0.963	-0.007	0.057
	$n = 6000$	-1.862	-0.653	0.024	0.700	1.646	0.950	-0.001	0.054
$\alpha = \alpha_0, \beta = \hat{\beta}_n$	$n = 4000$	-1.586	-0.578	0.022	0.695	1.799	0.948	0.005	0.068
	$n = 5000$	-1.440	-0.615	-0.006	0.696	1.648	0.959	0.001	0.058
	$n = 6000$	-1.653	-0.450	0.244	0.880	1.646	0.930	0.009	0.055
$\alpha = \hat{\alpha}_n, \beta = \hat{\beta}_n$	$n = 4000$	-1.572	-0.550	0.123	0.789	1.862	0.950	0.008	0.068
	$n = 5000$	-1.378	-0.541	0.097	0.798	1.782	0.957	0.007	0.059
	$n = 6000$	-1.659	-0.595	0.055	0.727	1.786	0.954	0.003	0.055
$ER = 0.9, v = 1.5$									
$\theta$									
$\alpha = \alpha_0, \beta = \beta_0$	$n = 4000$	-1.589	-0.595	-0.015	0.700	1.748	0.955	0.028	0.744
	$n = 5000$	-1.454	-0.668	-0.029	0.673	1.531	0.966	-0.006	0.638
	$n = 6000$	-1.701	-0.671	-0.098	0.572	1.747	0.940	-0.031	0.652
$\alpha = \alpha_0, \beta = 0.5\beta_0$	$n = 4000$	-0.026	0.961	1.579	2.307	3.369	0.675	1.205	1.434
	$n = 5000$	-0.117	0.805	1.443	2.165	3.003	3.705	0.978	1.183
	$n = 6000$	-0.371	0.705	1.327	1.957	3.189	0.764	0.813	1.037
$\alpha = \alpha_0, \beta = 2\beta_0$	$n = 4000$	-2.288	-1.288	-0.722	-0.002	1.009	0.886	-0.498	0.886
	$n = 5000$	-2.098	-1.348	-0.706	-0.010	0.858	0.916	-0.447	0.771
	$n = 6000$	-2.312	-1.309	-0.728	-0.050	1.071	0.887	-0.411	0.742
$\alpha = \alpha_0, \beta = \hat{\beta}_n$	$n = 4000$	-1.684	-0.599	0.092	0.751	1.805	0.934	0.058	0.780
	$n = 5000$	-1.468	-0.698	-0.003	0.696	1.641	0.966	0.007	0.658
	$n = 6000$	-1.670	-0.725	-0.068	0.660	1.775	0.931	-0.023	0.644
$\alpha = \hat{\alpha}_n, \beta = \hat{\beta}_n$	$n = 4000$	-1.532	-0.611	0.100	0.820	1.903	0.934	0.080	0.781
	$n = 5000$	-1.422	-0.584	0.050	0.746	1.745	0.959	0.049	0.664
	$n = 6000$	-1.498	-0.544	0.068	0.810	1.843	0.950	0.042	0.618

**Table S.3.** Percentiles of  $\zeta$  and CVG, bias, and RMSE of  $\hat{c}_n(\theta)$  when  $\alpha_0 = 5$ .

Settings		5%	25%	50%	75%	95%	CVG	bias	RMSE
$\mathcal{N}(0,1)$		-1.6449	-0.6749	0	0.6749	1.6449	0.95	0	
$ER = 0.6, v = 0.5$									
$\theta$									
$\alpha = \alpha_0, \beta = \beta_0$	$n = 4000$	-1.612	-0.659	-0.049	0.655	1.661	0.954	0.000	0.085
	$n = 5000$	-1.468	-0.636	-0.027	0.685	1.683	0.961	0.002	0.074
	$n = 6000$	-1.633	-0.560	0.079	0.723	1.751	0.940	0.003	0.070
$\alpha = \alpha_0, \beta = 0.5\beta_0$	$n = 4000$	-1.273	-0.289	0.319	1.010	2.038	0.942	0.030	0.091
	$n = 5000$	-1.183	-0.311	0.298	1.033	2.054	0.942	0.027	0.079
	$n = 6000$	-1.261	-0.245	0.401	1.023	2.070	0.932	0.025	0.074
$\alpha = \alpha_0, \beta = 2\beta_0$	$n = 4000$	-1.757	-0.829	-0.222	0.479	1.477	0.945	-0.015	0.086
	$n = 5000$	-1.616	-0.793	-0.191	-0.500	-1.520	0.958	-0.011	0.074
	$n = 6000$	-1.787	-0.709	-0.071	0.556	1.587	0.936	-0.007	0.070
$\alpha = \alpha_0, \beta = \hat{\beta}_n$	$n = 4000$	-1.607	-0.633	0.000	0.690	1.705	0.951	0.003	0.087
	$n = 5000$	-1.434	-0.591	0.030	0.719	1.766	0.953	0.005	0.075
	$n = 6000$	-1.609	-0.564	0.094	0.758	1.822	0.930	0.006	0.071
$\alpha = \hat{\alpha}_n, \beta = \hat{\beta}_n$	$n = 4000$	-1.556	-0.538	0.142	0.813	1.884	0.948	0.012	0.089
	$n = 5000$	-1.378	-0.514	0.116	0.835	1.762	0.958	0.010	0.076
	$n = 6000$	-1.530	-0.557	0.100	0.758	1.832	0.950	0.008	0.070
$ER = 0.6, v = 1.5$									
$\theta$									
$\alpha = \alpha_0, \beta = \beta_0$	$n = 4000$	-1.611	-0.651	-0.015	0.676	1.748	0.957	0.026	1.179
	$n = 5000$	-1.409	-0.606	0.052	0.727	1.705	0.958	0.069	1.031
	$n = 6000$	-1.346	-0.495	0.146	0.763	1.660	0.950	0.114	0.930
$\alpha = \alpha_0, \beta = 0.5\beta_0$	$n = 4000$	0.153	1.146	1.783	2.469	3.601	0.618	2.132	2.463
	$n = 5000$	0.109	1.070	1.720	2.432	3.475	0.628	1.818	2.113
	$n = 6000$	0.053	1.018	1.675	2.311	3.351	0.653	1.623	1.886
$\alpha = \alpha_0, \beta = 2\beta_0$	$n = 4000$	-2.308	-1.383	-0.802	-0.088	0.934	0.875	-0.877	1.456
	$n = 5000$	-2.093	-1.323	-0.675	0.004	0.964	0.909	-0.685	1.224
	$n = 6000$	-1.985	-1.186	-0.521	0.083	0.993	0.929	-0.538	1.059
$\alpha = \alpha_0, \beta = \hat{\beta}_n$	$n = 4000$	-1.664	-0.641	0.069	0.757	1.802	0.951	0.070	1.239
	$n = 5000$	-1.362	-0.615	0.080	0.792	1.788	0.956	0.105	1.074
	$n = 6000$	-1.368	-0.588	0.177	0.809	1.812	0.950	0.129	0.966
$\alpha = \hat{\alpha}_n, \beta = \hat{\beta}_n$	$n = 4000$	-1.528	-0.569	0.138	0.845	1.937	0.929	0.181	1.263
	$n = 5000$	-1.342	-0.522	0.105	0.838	1.822	0.956	0.150	1.065
	$n = 6000$	-1.468	-0.518	0.102	0.842	1.920	0.937	0.142	1.003
$ER = 0.9, v = 0.5$									
$\theta$									
$\alpha = \alpha_0, \beta = \beta_0$	$n = 4000$	-1.567	-0.602	-0.013	0.681	1.759	0.955	0.002	0.057
	$n = 5000$	-1.482	-0.664	-0.034	0.643	1.563	0.961	0.000	0.049
	$n = 6000$	-1.513	-0.615	0.077	0.637	1.745	0.953	0.002	0.045
$\alpha = \alpha_0, \beta = 0.5\beta_0$	$n = 4000$	-1.377	-0.423	0.179	0.871	1.956	0.947	0.013	0.058
	$n = 5000$	-1.333	-0.478	0.153	0.835	1.743	0.961	0.009	0.050
	$n = 6000$	-1.357	-0.468	0.233	0.800	1.894	0.947	0.009	0.046
$\alpha = \alpha_0, \beta = 2\beta_0$	$n = 4000$	-1.663	-0.708	-0.109	0.587	1.646	0.957	-0.004	0.057
	$n = 5000$	-1.554	-0.765	-0.121	0.556	1.465	0.958	-0.005	0.049
	$n = 6000$	-1.605	-0.692	-0.006	0.559	1.655	0.942	-0.002	0.045
$\alpha = \alpha_0, \beta = \hat{\beta}_n$	$n = 4000$	-1.571	-0.593	0.016	0.716	1.744	0.951	0.004	0.058
	$n = 5000$	-1.424	-0.653	-0.007	0.669	1.638	0.962	0.001	0.049
	$n = 6000$	-1.462	-0.572	0.095	0.704	1.803	0.949	0.003	0.045
$\alpha = \hat{\alpha}_n, \beta = \hat{\beta}_n$	$n = 4000$	-1.574	-0.539	0.106	0.803	1.853	0.952	0.007	0.059
	$n = 5000$	-1.327	-0.537	0.134	0.810	1.778	0.960	0.007	0.049
	$n = 6000$	-1.606	-0.601	0.058	0.713	1.756	0.956	0.003	0.046
$ER = 0.9, v = 1.5$									
$\theta$									
$\alpha = \alpha_0, \beta = \beta_0$	$n = 4000$	-1.574	-0.616	-0.015	0.661	1.764	0.955	0.009	0.345
	$n = 5000$	-1.414	-0.617	0.015	0.741	1.612	0.974	0.017	0.298
	$n = 6000$	-1.743	-0.591	0.066	0.677	1.795	0.933	0.008	0.292
$\alpha = \alpha_0, \beta = 0.5\beta_0$	$n = 4000$	-0.614	0.325	0.969	1.631	2.762	0.837	0.351	0.498
	$n = 5000$	-0.587	0.274	0.936	1.652	2.593	0.857	0.299	0.428
	$n = 6000$	-0.978	0.198	0.889	1.566	2.643	0.870	0.248	0.389
$\alpha = \alpha_0, \beta = 2\beta_0$	$n = 4000$	-1.988	-1.042	-0.448	0.234	1.285	0.933	-0.139	0.369
	$n = 5000$	-1.784	-1.013	-0.373	0.330	1.207	0.956	-0.105	0.313
	$n = 6000$	-2.094	-0.968	-0.301	0.312	1.420	0.925	-0.097	0.306
$\alpha = \alpha_0, \beta = \hat{\beta}_n$	$n = 4000$	-1.590	-0.609	0.029	0.720	1.791	0.943	0.021	0.356
	$n = 5000$	-1.364	-0.605	0.055	0.779	1.677	0.967	0.025	0.303
	$n = 6000$	-1.648	-0.608	0.107	0.709	1.823	0.947	0.015	0.296
$\alpha = \hat{\alpha}_n, \beta = \hat{\beta}_n$	$n = 4000$	-1.533	-0.549	0.113	0.849	1.836	0.940	0.047	0.369
	$n = 5000$	-1.387	-0.526	0.111	0.798	1.733	0.961	0.039	0.307
	$n = 6000$	-1.352	-0.534	0.110	0.765	1.755	0.956	0.039	0.281

**Table S.4.** Cross-validation results based on the Matérn covariance model and the new covariance model.

	Matérn class		New covariance class	
	$\nu = 0.5$	$\nu = 1.5$	$\nu = 0.5$	$\nu = 1.5$
$b$	411.1	411.1	411.0	411.0
$\sigma^2$	1.679	1.439	1.750	1.585
$\phi$	160.5	104.1	—	—
$\alpha$	—	—	0.381	0.353
$\beta$	—	—	6426.7	3439.9